

Secure SWIPT by Exploiting Constructive Interference and Artificial Noise

Muhammad R. A. Khandaker[✉], Senior Member, IEEE, Christos Masouros, Senior Member, IEEE, Kai-Kit Wong, Fellow, IEEE, and Stelios Timotheou, Senior Member, IEEE

Abstract—This paper studies interference exploitation techniques for secure beamforming design in simultaneous wireless information and power transfer in multiple-input single-output systems. In particular, multiuser interference (MUI) and artificially generated noise (AN) signals are designed as constructive to the information receivers (IRs) yet kept disruptive to potential eavesdropping by the energy receivers. The objective is to improve the received signal-to-interference and noise ratio (SINR) at the IRs by exploiting the MUI and AN power in an attempt to minimize the total transmit power. We first propose second-order cone programming-based solutions for the perfect channel state information (CSI) case by defining strong upper and lower bounds on the energy harvesting (EH) constraints. We then provide semidefinite programming-based solutions for the problems. In addition, we also solve the worst case harvested energy maximization problem under the proposed bounds. Finally, robust beamforming approaches based on the above are derived for the case of imperfect CSI. Our results demonstrate that the proposed constructive interference precoding schemes yield huge saving in transmit power over conventional interference management schemes. Most importantly, they show that, while the statistical constraints of conventional approaches may lead to instantaneous SINR as well as EH outages, the instantaneous constraints of our approaches guarantee both constraints at every symbol period.

Index Terms—SWIPT, energy harvesting, secure SWIPT, constructive interference, interference exploitation.

I. INTRODUCTION

SIMULTANEOUS wireless information and power transfer (SWIPT) has attracted a huge upsurge of interest in recent years due to its potential towards energy-efficient networks. SWIPT is particularly attractive in low energy-demanding scenarios to power battery-constrained wireless devices in which replacing or even recharging the battery is generally

Manuscript received December 31, 2017; revised June 7, 2018 and September 10, 2018; accepted September 24, 2018. Date of publication October 8, 2018; date of current version February 14, 2019. This work is supported by EPSRC under grant EP/M014150/1 and EP/R007934/1. The associate editor coordinating the review of this paper and approving it for publication was Y. P. Hong. (Corresponding author: Muhammad R. A. Khandaker.)

M. R. A. Khandaker is with the School of Engineering and Physical Sciences, Heriot-Watt University, Edinburgh EH14 4AS, U.K. (e-mail: m.khandaker@hw.ac.uk).

C. Masouros and K.-K. Wong are with the Department of Electronic and Electrical Engineering, University College London, London WC1E 7JE, U.K. (e-mail: c.masouros@ucl.ac.uk; kai-kit.wong@ucl.ac.uk).

S. Timotheou is with the Department of Electrical and Computer Engineering, University of Cyprus, 1678 Nicosia, Cyprus, and also with the KIOS Research Innovation Centre of Excellence, University of Cyprus, 1678 Nicosia, Cyprus (e-mail: timotheou.stelios@ucy.ac.cy).

Color versions of one or more of the figures in this paper are available online at <http://ieeexplore.ieee.org>.

Digital Object Identifier 10.1109/TCOMM.2018.2874658

difficult. However, conventional wireless transceivers that are optimal for information-only operation, may not be optimal for SWIPT since information and energy receivers operate at very different power sensitivity level [1]. Hence, a new set of optimization schemes are needed in order to make SWIPT practically appealing.

Since energy receivers (ERs) operate at significantly higher power level compared to information receivers (IRs), it is generally assumed that the receivers located within the vicinity of the transmitter are scheduled for energy harvesting (EH) while those located relatively further are intended for information transmission. Thus SWIPT becomes more viable in fifth-generation (5G) and beyond communication systems in which operators are expected to deploy a large number of base stations (BSs) in a smaller area even at a distance of tens of meters [2]. A key architectural design for 5G involves heterogeneous networks (HetNets), in which the BSs and the users are associated in multiple tiers with heterogeneous cell coverage areas. An inherent detrimental element in such network architectures is the co-tier and inter-tier interference. In fact, the sky-high spectral efficiency and energy efficiency envisaged in 5G communication networks vastly depends on appropriate interference management schemes [2]. However, as opposed to the conventional view of interference, we recognize that interference signals transport valuable energy to the ERs struggling to continue their operation due to insufficient power in stock. Thus ERs in future wireless networks may have access to higher power levels for energy scavenging. On the other hand, with access to stronger signals than the IRs, malicious ERs may pose potential security threats to the messages transmitted to the IRs. Thus developing appropriate security measures for SWIPT is also crucial [3], [4]. This motivates us to consider interference-aided security design for SWIPT communications in this paper.

Recently, a new branch of research has opened the window for data-aided beamforming for exploiting interference power in the downlink transmission [5]–[11]. The basic concept is to judiciously correlate interference signals among spatial streams rather than the conventional approach of fully decorrelating them. This constructive interference (CI) is designed on a per symbol basis and hence is modulation dependent. While most of the existing works on constructive interference focus on conventional downlink beamforming transmission [5]–[11], CI has been effectively used for physical layer security in [12], [13]. More recently, the authors of [14] and [15] considered a two-cell relay network, where each cell has one uplink and one downlink data traffic requirement. The proposed

interference alignment techniques in [14] align interference away from the useful signals by designing various transmit and receive schemes, whereas the schemes proposed in [16] exploit the overheard signals from the adjacent cell to improve the quality of signal reception in both cells. MMSE-based multiuser precoders have been proposed in [17] for reducing information leakage in a two-way relaying system. Note, however, that the above works consider different scenarios, either multicell communication or relay links, whereas our focus is on downlink transmission. More importantly, none of the above works designs explicit optimization formulations to exploit the interfering symbols and obtain a constructive (destructive) overlap with the expected signal at the IRs (Eves). Accordingly, these are distinct contributions to our work, whereas in our proposed schemes, we exploit the knowledge of data and CSI to develop more efficient secure precoding techniques. On the other hand, interference-aided SWIPT has been considered more recently in [18]. However, to the best of our knowledge, none of the above approaches considered exploiting interference for simultaneous information and power transmission, while securing the data from potential eavesdroppers.

In this paper, we consider a multiple-input single-output (MISO) downlink system where the transmitter aims at sending secret messages to a set of IRs, as well as wireless energy to a mutually exclusive group of ERs. Since the transmitter is required to secure the privacy of the IRs' messages, it needs to secure the message signals against potential eavesdropping by the ERs. Thus the ERs are legitimate users of the network for energy scavenging only. Our aim is to exploit the knowledge of multiuser interference (MUI) available at the transmitter as well as artificially generated noise (AN) signals for improving security in this SWIPT communication. Towards this end, we adjust the phase of the MUI and redesign AN signals in the form of constructive interference to the IRs while keeping these interferences disruptive to potential eavesdropping by the ERs. At the same time, the AN works as a vehicle for transporting energy. We aim at minimizing the total transmit power while guaranteeing the required SINR at the IRs as well as degrading the ERs' SINR below certain threshold. The energy harvesting requirements at the ERs are also guaranteed simultaneously. Note that the addition of security constraints introduces significant new challenges in the optimisation problem, which we will demonstrate in Section IV. The proposed constructive interference-based SWIPT precoding schemes offer fourfold benefits compared to conventional AN-based physical-layer security schemes considered in [19] and [20] as well as conventional secure SWIPT schemes designed in [3], [4], and [21]. Firstly, the constructive interference power greatly contributes to the received SINR at the IRs as opposed to the detrimental MUI in conventional interference management schemes. Secondly, to achieve a predefined level of SINR at the IRs, constructive interference based precoding scheme requires lower power compared to conventional precoding schemes thus reducing inter-user, inter-tier, and inter-cell interferences. Thirdly, the surplus power can be easily injected to the AN signal in order to boost the harvested energy at the ERs. Finally, since the proposed schemes work on a symbol-by-symbol basis, they can guarantee all the SINR, EH,

and secrecy constraints on an instantaneous basis, as opposed to conventional secure SWIPT that can lead to instantaneous signal or energy outages.¹

Both perfect and imperfect channel state information (CSI) cases have been investigated. The problem is non-convex in both cases, with second-order constraints. Although the SINR constraints considered in the power minimization problem can be transformed into convex conic constraints in closed form, the instantaneous (per symbol) EH constraints pose the biggest challenge² in exploiting interference for secure SWIPT. By defining strong upper and lower bounds on the EH constraints, we first propose second-order cone programming (SOCP) based solutions for the perfect CSI case. In order to investigate the tightness of the bounds, we then provide semi-definite programming (SDP) based solutions for the problems as benchmarks. Note that the SDP formulation has been proven very efficient in solving many non-convex problems [22]. In addition, we also solve the worst-case harvested energy maximization problem under the proposed bounds. Numerical simulations demonstrate that the proposed constructive interference precoding approaches yield superior performance over conventional schemes in terms of transmit power as well as harvested energy. For clarity, the contributions in this paper can be summarized as follows:

- 1) We first consider the case when CSI is perfectly known and design a phase-shift keying (PSK) modulation based secure precoding scheme such that the MUI and AN is constructive to the IR thus reducing the required transmit power for given quality-of-service (QoS) constraints. In order to tackle the non-convex energy harvesting constraints, we derive tight upper and lower bounds for the power minimization problem. SDP based solutions have also been derived for both upper and lower bounds.
- 2) Then, we derive a quadrature-amplitude modulation (QAM) based secure precoding scheme for multi-level modulations.
- 3) Finally, we design worst-case robust secure precoders for SWIPT in the presence of imperfect CSI of all the nodes for both PSK and QAM modulations.

In all cases, the proposed schemes outperform the conventional AN-aided secure precoding schemes.

The rest of this paper is organized as follows. In Section II, the system model of a secret MISO downlink system for SWIPT is introduced. The conventional SINR-constrained power minimization problem is discussed in Section III for the perfect CSI case whereas in Section IV, constructive AN-based solutions to the same problem have been devised for secure SWIPT. Next, we extend the analyses to QAM constellation schemes in Section VI considering perfect CSI. Finally, in Section VII, we develop robust constructive interference precoding schemes for both PSK and QAM modulations. Section VIII presents the simulation results that justify the significance of the proposed algorithms under various scenarios. Concluding remarks are provided in Section IX.

¹This is demonstrated through computer simulations in Section VIII.

²The exact technical challenge will be illustrated later in Section IV.

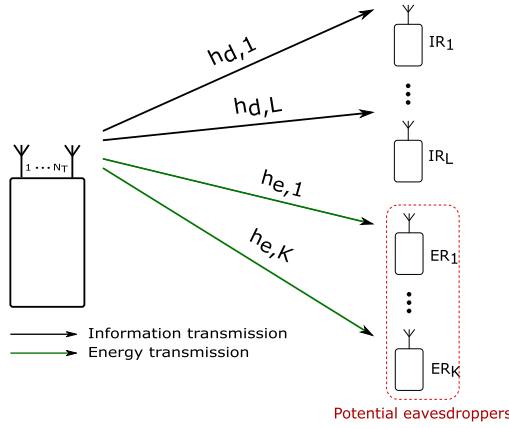


Fig. 1. System model for secure SWIPT with untrusted energy receivers.

II. SYSTEM MODEL

We consider a MISO downlink system where the transmitter (BS) equipped with N_T transmit antennas intends to transmit secret information to L IRs as well as wireless power to K ERs. Note that the BS plays a hybrid role transmitting both energy and information, as opposed to separate power beacons and information transmitters for powering the energy scavenging nodes considered in [23]. The IR and Eves are all equipped with a single antenna.³ We also assume that the IRs are trustworthy for information reception, whereas the ERs are trustworthy for energy harvesting only. It may happen in practice, however, that some of the ERs are inquisitive to the secret messages transmitted to the IRs and intend to overhear the information signal. Thus, the BS needs to deploy appropriate mechanisms to block potential eavesdropping by the ERs. Hence in order to keep the ERs blind about the secret messages, the BS injects AN signals into the transmit signal in an attempt to reduce the received SINRs at the ERs. Thus the received signal at the l th IR and that at the k th ER are given, respectively, by $y_{d,l}$ and $y_{e,k}$:

$$y_{d,l} = \mathbf{h}_{d,l}^T \mathbf{x} + n_{d,l}, \text{ for } l = 1, \dots, L, \quad (1)$$

$$y_{e,k} = \mathbf{h}_{e,k}^T \mathbf{x} + n_{e,k}, \text{ for } k = 1, \dots, K, \quad (2)$$

where $\mathbf{h}_{d,l}$ and $\mathbf{h}_{e,k}$ are the $N_T \times 1$ complex channel vectors between the BS and the l th IR and between the BS and the k th Eve, respectively, $n_{d,l} \sim \mathcal{CN}(0, \sigma_d^2)$ and $n_{e,k} \sim \mathcal{CN}(0, \sigma_e^2)$ are the additive Gaussian noises at the l th IR and the k th Eve, respectively. The BS chooses the $N_T \times 1$ transmit signal vector \mathbf{x} as the sum of information beamforming vectors $\mathbf{b}_{d,l} s_{d,l}$, $l = 1, \dots, L$, and the $N_T \times 1$ AN vector \mathbf{z} such that the baseband transmit signal is given by

$$\mathbf{x} = \sum_{l=1}^L \mathbf{b}_{d,l} s_{d,l} + \mathbf{z}, \quad (3)$$

³Since our intention is to present the proposed constructive interference based secure precoding schemes to the readers in an *easy-to-access* manner, we restrict our analysis to the MISO eavesdropping scenario. However, for the general MIMO eavesdropping case, the generalization is straightforward by replacing the vector channels with matrices. As such, one needs to concatenate the channel matrices into vectors and do minor modifications in the required transformations to formulate the proposed SOCP solutions.

where $s_{d,l} = e^{j\phi_{d,l}} \sim \mathcal{CN}(0, 1)$ is the unit-amplitude confidential information-bearing symbol for the l th IR.

Accordingly, the received SINR at the l th IR is given by

$$\Gamma_{d,l} = \frac{|\mathbf{h}_{d,l}^T \mathbf{b}_{d,l}|^2}{\sum_{m=1, m \neq l}^L |\mathbf{h}_{d,l}^T \mathbf{b}_{d,m}|^2 + |\mathbf{h}_{d,l}^T \mathbf{z}|^2 + \sigma_d^2}, \quad (4)$$

and that at the k th ER intending to wiretap the l th IR's signal is given by

$$\Gamma_{e,k}^{(l)} = \frac{|\mathbf{h}_{e,k}^T \mathbf{b}_{d,l}|^2}{\sum_{m=1, m \neq l}^L |\mathbf{h}_{e,k}^T \mathbf{b}_{d,m}|^2 + |\mathbf{h}_{e,k}^T \mathbf{z}|^2 + \sigma_e^2}, \quad \forall l, \forall k. \quad (5)$$

On the other hand, the average harvested power (i.e., harvested energy per unit time) at the k th ER can be expressed as

$$P_{h,k}^{\text{avg}} = \xi \left(\sum_{l=1}^L |\mathbf{h}_{e,k}^T \mathbf{b}_{d,l}|^2 + |\mathbf{h}_{e,k}^T \mathbf{z}|^2 + \sigma_e^2 \right), \quad (6)$$

where ξ is the conversion efficiency of the energy transducers from RF domain to electrical domain.

III. CONVENTIONAL AVERAGE POWER MINIMIZATION

In this section, we assume that perfect CSI of all nodes is available at the transmitter. This is practicable in the considered system model since both the IRs and the ERs are legitimate users of the system for different services namely information and energy, respectively. We consider a power minimization problem for secure transmission of information to the IRs under QoS constraints at the IRs as well as secrecy constraints at the untrusted ERs (with respect to information) while sustaining their energy harvesting requirements [4]. In order to satisfy these requirements, the conventional power minimization problem (in statistical sense) is formulated as [3]

$$\min_{\{\mathbf{b}_{d,l}\}, \mathbf{z}} \sum_{l=1}^L \|\mathbf{b}_{d,l}\|^2 + \|\mathbf{z}\|^2 \quad (7a)$$

$$\text{s.t. } \frac{|\mathbf{h}_{d,l}^T \mathbf{b}_{d,l}|^2}{\sum_{m=1, m \neq l}^L |\mathbf{h}_{d,l}^T \mathbf{b}_{d,m}|^2 + |\mathbf{h}_{d,l}^T \mathbf{z}|^2 + \sigma_d^2} \geq \gamma_d, \quad \forall l, \quad (7b)$$

$$\frac{|\mathbf{h}_{e,k}^T \mathbf{b}_{d,l}|^2}{\sum_{m=1, m \neq l}^L |\mathbf{h}_{e,k}^T \mathbf{b}_{d,m}|^2 + |\mathbf{h}_{e,k}^T \mathbf{z}|^2 + \sigma_e^2} \leq \gamma_e, \quad \forall k, \forall l, \quad (7c)$$

$$\xi \left(\sum_{l=1}^L |\mathbf{h}_{e,k}^T \mathbf{b}_{d,l}|^2 + |\mathbf{h}_{e,k}^T \mathbf{z}|^2 + \sigma_e^2 \right) \geq \eta_k, \quad \forall k, \quad (7d)$$

where γ_d is the minimum SINR requirement for correct detection at the IRs and γ_e is the secrecy threshold for the ERs interception, whereas η_k is the energy harvesting threshold at the k th ER. The power minimization problem (7) is non-convex and has been solved considering various system configurations [3], [4]. We consider the schemes proposed in [3], [4] as the benchmark schemes. One conventional approach

is to reformulate problem (7) as an SDP and optimize the transmit covariance matrices for information and AN signals. However, this results in inherent rank constraints on the information covariance matrices. Conventionally, the non-convex rank constraints are dropped so that the relaxed problem can be solved using existing SDP solvers [24]. Interestingly, it has been proven in [3] and [4] that for a wide range of practically representative scenarios, the original problem can be solved optimally satisfying the rank constraints. Interested readers are referred to [3] and [4] for further details on the technique. Although the solutions proposed in [3] and [4] are optimal from a stochastic viewpoint, the hidden power in the AN signals has been treated as detrimental for the desired information at the IRs, and hence, either nullified or suppressed. In the following section, we endeavour to develop precoding schemes exploiting the MUI and AN power constructively for the desired signal at the IRs.

IV. CONSTRUCTIVE AN-BASED INSTANTANEOUS POWER MINIMIZATION

By exploiting MUI on a symbol-by-symbol basis, it has been shown in [3] and [4] that the MUI power can significantly contribute towards the received SINR at the desired receiver. The theory and characterization criteria for this constructive interference have been extensively studied in [5]–[9] and [25]. To avoid repetition, we refer the reader to the above works for the details, while here we employ this concept directly to design our secure beamforming problems for SWIPT.

Constructive IR Constraints: As in many conventional beamforming schemes, we assume in this section that full CSI of all nodes is available at the transmitter.⁴ We aim at exploiting the available knowledge of MUI as well as AN to boost the received SINR at the IR in an attempt to reduce the required transmit power, while guaranteeing the secrecy and EH constraints for the ERs. We restrict our analysis in this section to M -PSK modulation, while extension to other modulation schemes (e.g., M -QAM) is relegated until Section VI. Now, the MUI and AN signals will be constructive to the received signal at the IR if they move the received symbols away from the decision thresholds of the constellation. These are represented by the red dashed lines in Fig. 2 for the example of 8-PSK constellation. This can be effectively done by pushing the decision symbols towards the constructive regions of the modulation constellation, denoted by the green shaded areas in Fig. 2. Hence we intend to keep the angle of the received signal aligned with the angle of the corresponding desired symbol $s_{d,l}$ by appropriately designing the transmit and AN beamforming vectors.⁵

In order to align the transmit symbols along the direction of the l th IR's modulated symbol $s_{d,l}$, we can subtract the

⁴Secure beamforming design with imperfect CSI will be studied in Section VII.

⁵Although we selected 8-PSK as a representative modulation scheme for exposition in Fig. 2, the proposed algorithms are readily applicable to any PSK modulation scheme. Indeed, all formulations shown are applicable to any order PSK modulation, parametric to the angle θ .

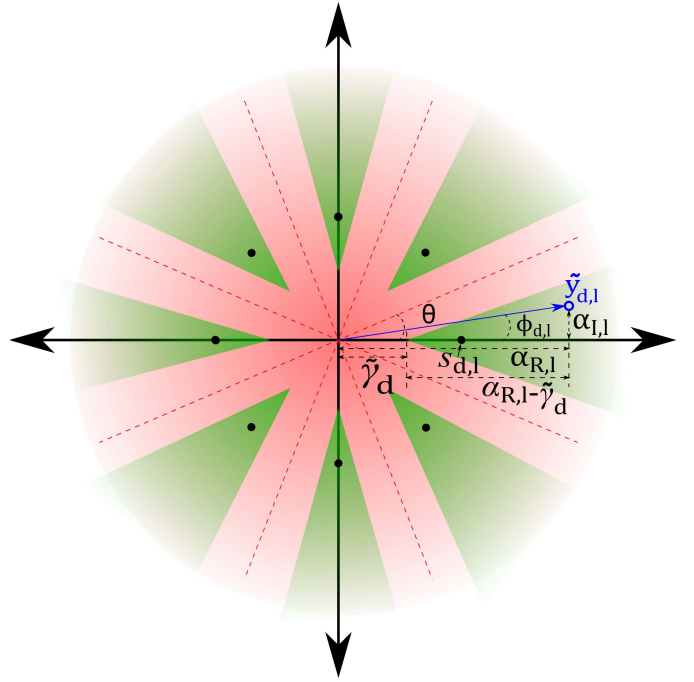


Fig. 2. Constructive interference design for IR with 8-PSK modulation. The decision thresholds are represented by the red dashed lines and the constructive regions are denoted by the green shaded areas. The constructive interference signals move the received symbols at the IR ($\tilde{y}_{d,l}$) away from the decision thresholds of the constellation towards the constructive region of the constellation point of interest. In contrast, the AN signals destructive to the eavesdroppers push the eavesdroppers' received signals away from the constellation point of interest.

phase of $s_{d,l}$ from the phase of the corresponding information-bearing symbol. As such, the transmit signal \mathbf{x} can be expressed as

$$\mathbf{x} = \sum_{m=1}^L \mathbf{b}_{d,m} e^{j(\phi_{d,m} - \phi_{d,l})} s_{d,l} + \mathbf{z} e^{-j\phi_{d,l}} s_{d,l}. \quad (8)$$

Although in (8), the transmit symbol has been aligned with the l -th IR, in general, any of the user's signal can be chosen as the reference signal. Assuming constant envelop transmission, the instantaneous transmit power is given by

$$P_T = \left\| \sum_{m=1}^L \mathbf{b}_{d,m} e^{j(\phi_{d,m} - \phi_{d,l})} + \mathbf{z} e^{-j\phi_{d,l}} \right\|^2, \quad (9)$$

and the instantaneous harvested power at the k th ER is given by

$$P_{h,k}^{\text{ins}} = \left| \mathbf{h}_{e,k}^T \left(\sum_{m=1}^L \mathbf{b}_{d,m} e^{j(\phi_{d,m} - \phi_{d,l})} + \mathbf{z} e^{-j\phi_{d,l}} \right) \right|^2. \quad (10)$$

Note that in (8) - (10), any of the IRs' symbols can be taken as the reference (l) without loss of generality.

For constructive precoding, the MUI and AN signals received at the IRs are not suppressed or nullified in contrast to their conventional use (cf. Section III), rather optimized instantaneously such that they contribute to the received signal power. Following the constructive interference characterization

criteria derived in [8] and [9], it can be shown that the received SINR (4) at the l th IR can be rewritten as

$$\Gamma_{d,l} = \frac{\left| \mathbf{h}_{d,l}^T \left(\sum_{m=1}^L \mathbf{b}_{d,m} s_{d,m} + \mathbf{z} \right) \right|^2}{\sigma_d^2}. \quad (11)$$

Clearly, it is evident from (11) that the MUI as well as the AN are now contributing to the desired signal power. Thus the received SINR at the IR has effectively turned to SNR after applying constructive precoding. However, the SINR at the k th ER remains the same as in (5) since no interference/AN signal has been made constructive to the ERs.

Now, our target is to design the signal and AN beamforming vectors such that the constructive SINR (11) becomes achievable at the IRs. Let us denote $\tilde{y}_{d,l} \triangleq \mathbf{h}_{d,l}^T \left(\sum_{m=1}^L \mathbf{b}_{d,m} e^{j(\phi_{d,m} - \phi_{d,l})} + \mathbf{z} e^{-j\phi_{d,l}} \right)$ as the received signal ignoring the AWGN at the l th IR, and $\alpha_{R,l}$ and $\alpha_{I,l}$ as the abscissa and the ordinate of the phase-adjusted signal $\tilde{y}_{d,l}$, respectively. Applying basic geometric principles to Fig. 2, it can be observed that the interference contaminated received signal $\tilde{y}_{d,l}$ lays on the constructive zone of the desired symbol $s_{d,l}$ as long as the following condition is satisfied

$$-\theta \leq \phi_{d,l} \leq \theta, \quad \text{i.e., } \frac{|\alpha_{I,l}|}{\alpha_{R,l} - \tilde{\gamma}_d} \leq \tan \theta, \quad (12)$$

where $\theta = \pi/M$, M is the constellation size and $\tilde{\gamma}_d \triangleq \sigma_d \sqrt{\Gamma_d}$. Thus the SINR constraint (7b) can be expressed as the following constraint [9]

$$\begin{aligned} & \left| \Im \left\{ \mathbf{h}_{d,l}^T \left(\sum_{m=1}^L \mathbf{b}_{d,m} e^{j(\phi_{d,m} - \phi_{d,l})} + \mathbf{z} e^{-j\phi_{d,l}} \right) \right\} \right| \\ & \leq \left[\Re \left\{ \mathbf{h}_{d,l}^T \left(\sum_{m=1}^L \mathbf{b}_{d,m} e^{j(\phi_{d,m} - \phi_{d,l})} + \mathbf{z} e^{-j\phi_{d,l}} \right) \right\} \right. \\ & \quad \left. - \sigma_{d,l} \sqrt{\gamma_d} \tan \theta, \right] \end{aligned} \quad (13)$$

where $\Re\{x\}$ and $\Im\{x\}$ indicate the real and imaginary parts of the complex number x , respectively.

Note that the phases of the MUI and the AN signals in (13) have been shifted by the phase of the desired symbol $s_{d,l}$. We note that this signal alignment will only hold for the structure of the l th IR's channel $\mathbf{h}_{d,l}$, while there will be no such alignment for the ERs' channels $\mathbf{h}_{e,k}$, $k = 1, \dots, K$, which are assumed statistically independent.

Destructive Eavesdropping Constraints: Now, we deal with the instantaneous eavesdropping constraint. The aim is to design the signal and AN beamformers such that the MUI and AN signals are as disruptive as possible to the ERs' detection while satisfying their instantaneous EH constraints. As long as the ERs' channel knowledge is available at the transmitter, one can do so by pushing the received signals at the ERs away from the decision thresholds (towards the corresponding red zone in Fig. 2, i.e., $|\phi_{e,k}| \geq \theta$). This makes correct detection more challenging for the ERs by reducing the received SINR. The benefit is that the given secrecy constraints can be guaranteed on a symbol-by-symbol basis, rather than the conventional

statistical guarantees [3], [4], which are prone to instantaneous outages.⁶

Thus the SINR restriction constraints at the ERs can be represented by the following system of inequalities

$$\begin{aligned} & -\Im \left\{ \mathbf{h}_{e,k}^T \left(\sum_{m=1}^L \mathbf{b}_{d,m} e^{j(\phi_{d,m} - \phi_{d,l})} + \mathbf{z} e^{-j\phi_{d,l}} \right) \right\} \\ & \leq \left(\Re \left\{ \mathbf{h}_{e,k}^T \left(\sum_{m=1}^L \mathbf{b}_{d,m} e^{j(\phi_{d,m} - \phi_{d,l})} + \mathbf{z} e^{-j\phi_{d,l}} \right) \right\} \right. \\ & \quad \left. - \sigma_e \sqrt{\gamma_e} \tan \theta, \quad \forall k. \right) \end{aligned} \quad (14a)$$

$$\begin{aligned} & \Im \left\{ \mathbf{h}_{e,k}^T \left(\sum_{m=1}^L \mathbf{b}_{d,m} e^{j(\phi_{d,m} - \phi_{d,l})} + \mathbf{z} e^{-j\phi_{d,l}} \right) \right\} \\ & \geq \left(\Re \left\{ \mathbf{h}_{e,k}^T \left(\sum_{m=1}^L \mathbf{b}_{d,m} e^{j(\phi_{d,m} - \phi_{d,l})} + \mathbf{z} e^{-j\phi_{d,l}} \right) \right\} \right. \\ & \quad \left. - \sigma_e \sqrt{\gamma_e} \tan \theta, \quad \forall k. \right) \end{aligned} \quad (14b)$$

Thus exploiting the knowledge of the interfering signals (MUI and AN in this case), the constructive precoding design problem with the secrecy power minimization objective can be formulated as

$$\min_{\{\mathbf{b}_{d,l}\}, \mathbf{z}} \left\| \sum_{m=1}^L \mathbf{b}_{d,m} e^{j(\phi_{d,m} - \phi_{d,l})} + \mathbf{z} e^{-j\phi_{d,l}} \right\|^2 \quad (15a)$$

$$\text{s.t. Constraints (14a) and (14b) satisfied,} \quad (15b)$$

$$\begin{aligned} & \left| \Im \left\{ \mathbf{h}_{d,l}^T \left(\sum_{m=1}^L \mathbf{b}_{d,m} e^{j(\phi_{d,m} - \phi_{d,l})} + \mathbf{z} e^{-j\phi_{d,l}} \right) \right\} \right| \\ & \leq \left(\Re \left\{ \mathbf{h}_{d,l}^T \left(\sum_{m=1}^L \mathbf{b}_{d,m} e^{j(\phi_{d,m} - \phi_{d,l})} + \mathbf{z} e^{-j\phi_{d,l}} \right) \right\} \right. \\ & \quad \left. - \sigma_d \sqrt{\gamma_d} \tan \theta, \quad \forall l, \right) \end{aligned} \quad (15c)$$

$$\left| \mathbf{h}_{e,k}^T \left(\sum_{m=1}^L \mathbf{b}_{d,m} e^{j(\phi_{d,m} - \phi_{d,l})} + \mathbf{z} e^{-j\phi_{d,l}} \right) \right|^2 \geq \bar{\eta}_k, \quad \forall k, \quad (15d)$$

where $\bar{\eta}_k \triangleq \eta_k / \xi, \forall k$.

For notational simplicity, let us now define $N_T \times 1$ vectors $\tilde{\mathbf{h}}_{d,l} \triangleq \mathbf{h}_{d,l} e^{j(\phi_{d,1} - \phi_{d,l})}$, $\tilde{\mathbf{h}}_{e,k} \triangleq \mathbf{h}_{e,k} e^{j(\phi_{d,1} - \phi_{d,l})}$, and $\mathbf{w} \triangleq \sum_{m=1}^L \mathbf{b}_{d,m} e^{j(\phi_{d,m} - \phi_{d,l})} + \mathbf{z} e^{-j\phi_{d,l}}$. Then the problem (15) can be represented as the following instantaneous secrecy power minimization problem for SWIPT:

$$\min_{\mathbf{w}} \|\mathbf{w}\|^2 \quad (16a)$$

$$\text{s.t. } \left| \Im \left\{ \tilde{\mathbf{h}}_{d,l}^T \mathbf{w} \right\} \right| \leq \left(\Re \left\{ \tilde{\mathbf{h}}_{d,l}^T \mathbf{w} \right\} - \sigma_d \sqrt{\gamma_d} \right) \tan \theta, \quad \forall l, \quad (16b)$$

$$\Im \left\{ \tilde{\mathbf{h}}_{e,k}^T \mathbf{w} \right\} \geq \left(\Re \left\{ \tilde{\mathbf{h}}_{e,k}^T \mathbf{w} \right\} - \sigma_e \sqrt{\gamma_e} \right) \tan \theta, \quad \forall k, \quad (16c)$$

$$-\Im \left\{ \tilde{\mathbf{h}}_{e,k}^T \mathbf{w} \right\} \leq \left(\Re \left\{ \tilde{\mathbf{h}}_{e,k}^T \mathbf{w} \right\} - \sigma_e \sqrt{\gamma_e} \right) \tan \theta, \quad \forall k, \quad (16d)$$

$$\left\| \tilde{\mathbf{h}}_{e,k}^T \mathbf{w} \right\|^2 \geq \bar{\eta}_k, \quad \forall k. \quad (16e)$$

⁶This is demonstrated through numerical simulations in Section VIII.

Note that the problem (16) forms a virtual multicasting secrecy optimization problem for SWIPT with only one vector variable \mathbf{w} to be optimized. Apparently, problem (16) looks simpler. However, the problem is in fact nonconvex due to the EH constraint (16e) and the solution to this problem is not tractable. The main challenge arises from the fact that the instantaneous EH constraint (16e) cannot be convexified using standard optimization techniques in closed form. In conventional optimization schemes for SWIPT, the EH constraint is generally transformed to a trace (of a matrix) constraint, which is convex [3], [4], [21]. However, this cannot be straightforwardly applied to the data-aided instantaneous EH constraint (16e). Hence in the following, we endeavour to develop SOCP based approximate solutions for problem (16) by defining appropriate bounds.

A. SOCP Upper Bound Solution

In order to obtain an upper bounding solution to problem (16) we need to approximate the non-convex constraint (16e) with a convex one that always satisfies (16e). From (16c), we have

$$\Im\{\tilde{\mathbf{h}}_{e,k}^T \mathbf{w}\} \geq (\Re\{\tilde{\mathbf{h}}_{e,k}^T \mathbf{w}\} - \sigma_e \sqrt{\gamma_e}) \tan \theta \geq 0, \quad \forall k. \quad (17)$$

Thus in order to bound (16e), we consider the inequality

$$\Im\{\tilde{\mathbf{h}}_{e,k}^T \mathbf{w}\} \geq \Re\{\tilde{\mathbf{h}}_{e,k}^T \mathbf{w}\} \tan \theta. \quad (18)$$

Because $\Re\{\tilde{\mathbf{h}}_{e,k}^T \mathbf{w}\} \tan \theta \geq (\Re\{\tilde{\mathbf{h}}_{e,k}^T \mathbf{w}\} - \sigma_e \sqrt{\gamma_e}) \tan \theta$, it is true that whenever (18) holds, inequality (17) holds as well since $\sigma_e \sqrt{\gamma_e}$ is nonnegative. Combining inequality (18) with $\|\tilde{\mathbf{h}}_{e,k}^T \mathbf{w}\|^2$ yields

$$\begin{aligned} \|\tilde{\mathbf{h}}_{e,k}^T \mathbf{w}\|^2 &= \Re\{\tilde{\mathbf{h}}_{e,k}^T \mathbf{w}\}^2 + \Im\{\tilde{\mathbf{h}}_{e,k}^T \mathbf{w}\}^2 \geq \Re\{\tilde{\mathbf{h}}_{e,k}^T \mathbf{w}\}^2 \\ &\quad + \Im\{\tilde{\mathbf{h}}_{e,k}^T \mathbf{w}\} \Re\{\tilde{\mathbf{h}}_{e,k}^T \mathbf{w}\} \tan \theta \end{aligned} \quad (19)$$

so that we can replace (16e) with

$$\Re\{\tilde{\mathbf{h}}_{e,k}^T \mathbf{w}\} (\Re\{\tilde{\mathbf{h}}_{e,k}^T \mathbf{w}\} + \Im\{\tilde{\mathbf{h}}_{e,k}^T \mathbf{w}\} \tan \theta) \geq \bar{\eta}_k, \quad \forall k. \quad (20)$$

Note that (20) is a stricter constraint compared to (16e). Thus replacing (16e) by (20) will provide an upper bound solution for problem (16). Although (20) is still non-convex, it can be transformed into a convex constraint by defining two positive real-valued slack variables $r_{1,k} \geq 0, r_{2,k} \geq 0, \forall k$ such that:

$$r_{1,k} = \Re\{\tilde{\mathbf{h}}_{e,k}^T \mathbf{w}\} \quad (21)$$

$$r_{2,k} = \Re\{\tilde{\mathbf{h}}_{e,k}^T \mathbf{w}\} + \Im\{\tilde{\mathbf{h}}_{e,k}^T \mathbf{w}\} \tan \theta \quad (22)$$

$$r_{1,k} r_{2,k} \geq \bar{\eta}_k, \quad \forall k. \quad (23)$$

Constraint (23) is a restricted hyperbolic constraint of the form $yz \geq x^2, y, z \geq 0$, with $y = r_{1,k}$, $z = r_{2,k}$ and $x = \sqrt{\eta_k}$, which is equivalent to the convex rotated second-order cone (SOC) constraint [22]

$$\left\| \begin{bmatrix} 2x \\ y - z \end{bmatrix} \right\| \leq y + z. \quad (24)$$

By transforming the EH constraint (23) into a rotated SOC constraint and enforcing (17), problem (16) becomes

$$\min_{\mathbf{w}, r_{1,k}, r_{2,k}} \|\mathbf{w}\|^2 \quad (25a)$$

$$\text{s.t. } \left| \Im\{\tilde{\mathbf{h}}_{d,l}^T \mathbf{w}\} \right| \leq (\Re\{\tilde{\mathbf{h}}_{d,l}^T \mathbf{w}\} - \sigma_e \sqrt{\gamma_e}) \tan \theta, \quad \forall l, \quad (25b)$$

$$\Im\{\tilde{\mathbf{h}}_{e,k}^T \mathbf{w}\} \geq (\Re\{\tilde{\mathbf{h}}_{e,k}^T \mathbf{w}\}) \tan \theta, \quad \forall k, \quad (25c)$$

$$-\Im\{\tilde{\mathbf{h}}_{e,k}^T \mathbf{w}\} \leq (\Re\{\tilde{\mathbf{h}}_{e,k}^T \mathbf{w}\} - \sigma_e \sqrt{\gamma_e}) \tan \theta, \quad \forall k, \quad (25d)$$

$$r_{1,k} = \Re\{\tilde{\mathbf{h}}_{e,k}^T \mathbf{w}\}, \quad \forall k, \quad (25e)$$

$$r_{2,k} = \Re\{\tilde{\mathbf{h}}_{e,k}^T \mathbf{w}\} + \Im\{\tilde{\mathbf{h}}_{e,k}^T \mathbf{w}\} \tan \theta, \quad \forall k, \quad (25f)$$

$$\left\| \begin{bmatrix} 2\sqrt{\eta_k} \\ r_{1,k} - r_{2,k} \end{bmatrix} \right\| \leq r_{1,k} + r_{2,k}, \quad \forall k, \quad (25g)$$

$$r_{1,k} \geq 0, \quad r_{2,k} \geq 0, \quad \forall k. \quad (25h)$$

Note that problem (25) is now convex and can be optimally solved using existing SOCP solvers [24]. In addition, notice that constraints (16c) and (16e) has been replaced by (25c) and (25e) - (25h), which always satisfy the original constraints according to (18) and (19), respectively. Hence, the optimal solution of (25) provides an upper bound to the original problem.

B. SOCP Lower Bound Solution

In order to obtain a lower bound solution to problem (16), we bound the non-convex constraint (16e) from below. This can be achieved by relaxing the energy harvesting constraint (16e). Now, inequalities (16c) and (16d), respectively, state that

$$\Im\{\tilde{\mathbf{h}}_{e,k}^T \mathbf{w}\} \geq (\Re\{\tilde{\mathbf{h}}_{e,k}^T \mathbf{w}\} - \sigma_e \sqrt{\gamma_e}) \tan \theta, \quad (26)$$

$$-\Im\{\tilde{\mathbf{h}}_{e,k}^T \mathbf{w}\} \leq (\Re\{\tilde{\mathbf{h}}_{e,k}^T \mathbf{w}\} - \sigma_e \sqrt{\gamma_e}) \tan \theta. \quad (27)$$

Hence, it is true that $\Im\{\tilde{\mathbf{h}}_{e,k}^T \mathbf{w}\} \geq 0$, and we have

$$\begin{aligned} \sigma_e \sqrt{\gamma_e} - \Im\{\tilde{\mathbf{h}}_{e,k}^T \mathbf{w}\} / \tan \theta &\leq \Re\{\tilde{\mathbf{h}}_{e,k}^T \mathbf{w}\} \leq \Im\{\tilde{\mathbf{h}}_{e,k}^T \mathbf{w}\} / \tan \theta \\ &\quad + \sigma_e \sqrt{\gamma_e} \end{aligned} \quad (28)$$

Combining the fact that $\Re\{\tilde{\mathbf{h}}_{e,k}^T \mathbf{w}\} \leq \Im\{\tilde{\mathbf{h}}_{e,k}^T \mathbf{w}\} / \tan \theta + \sigma_e \sqrt{\gamma_e}$ with (16e) yields

$$(\Im\{\tilde{\mathbf{h}}_{e,k}^T \mathbf{w}\} / \tan \theta + \sigma_e \sqrt{\gamma_e})^2 + \Im\{\tilde{\mathbf{h}}_{e,k}^T \mathbf{w}\}^2 \geq \bar{\eta} \quad (29)$$

$$\begin{aligned} \Im\{\tilde{\mathbf{h}}_{e,k}^T \mathbf{w}\}^2 (1 + \frac{1}{\tan^2 \theta}) + \Im\{\tilde{\mathbf{h}}_{e,k}^T \mathbf{w}\} \frac{2\sigma_e \sqrt{\gamma_e}}{\tan \theta} + \sigma_e \sqrt{\gamma_e} \\ - \bar{\eta} \geq 0. \end{aligned} \quad (30)$$

Essentially, due to inequality (28), it is true that

$$\begin{aligned} (\Im\{\tilde{\mathbf{h}}_{e,k}^T \mathbf{w}\} / \tan \theta + \sigma_e \sqrt{\gamma_e})^2 + \Im\{\tilde{\mathbf{h}}_{e,k}^T \mathbf{w}\}^2 &\geq \Re\{\tilde{\mathbf{h}}_{e,k}^T \mathbf{w}\}^2 \\ &\quad + \Im\{\tilde{\mathbf{h}}_{e,k}^T \mathbf{w}\}^2. \end{aligned} \quad (31)$$

Note that (31) is a second-order inequality, which is solvable when the discriminant is non-negative. This observation leads to the following condition:

$$\Delta_k = 4\bar{\eta}_k (1 + \frac{1}{\tan^2 \theta}) - 4\sigma_e^2 \gamma_e \geq 0. \quad (32)$$

Under condition (32) and given the fact that $\Im\{\tilde{\mathbf{h}}_{e,k}^T \mathbf{w}\} \geq 0$, inequality (30) can be simplified to

$$\Im\{\tilde{\mathbf{h}}_{e,k}^T \mathbf{w}\} \geq \frac{-\sigma_e \sqrt{\gamma_e} / \tan \theta + \sqrt{\bar{\eta}_k (1 + 1 / \tan^2 \theta)} - \sigma_e^2 \gamma_e}{1 + 1 / \tan^2 \theta} \quad (33)$$

Note that it is possible that condition (33) is bounded from below. Thus condition (33) can be used as a lower bound instead of the inequality (16e). Accordingly, the lower bound problem is formulated as

$$\min_{\mathbf{w}} \|\mathbf{w}\|^2 \quad (34a)$$

$$\text{s.t. Constraints (16b), (16c), (16d),} \quad (34b)$$

$$\text{constraint (33) whenever } \Delta_k \geq 0, \quad (34c)$$

which is a linear programming problem. Problem (34) can be optimally solved using existing convex optimization toolboxes [24].

V. SDP-BASED SOLUTIONS

Any SOCP constraint of the form $x^2 \leq yx, y, z \geq 0$ can be transformed into an SDP constraint according to the following lemma [22]:

$$x^2 \leq yx, y, z \geq 0 \Leftrightarrow \begin{bmatrix} y & x \\ x & z \end{bmatrix} \succeq \mathbf{0}. \quad (35)$$

We apply this lemma in order to derive corresponding SDP solutions for the problems (25) and (34).

A. SDP Upper Bound Solution

In this subsection, we provide the SDP upper bound solution of (25) for completeness. In the SDP formulation, we do not need to define any slack variable, e.g., $r_{1,k}, r_{2,k}$. Thus we obtain the SDP formulation of problem (25) as

$$\min_{\mathbf{w}} \|\mathbf{w}\|^2 \quad (36a)$$

$$\text{s.t. Constraint (25b) -- (25d),} \quad (36b)$$

$$\begin{bmatrix} \Re\{\tilde{\mathbf{h}}_{e,k}^T \mathbf{w}\} & \sqrt{\bar{\eta}_k} \\ \sqrt{\bar{\eta}_k} & \Re\{\tilde{\mathbf{h}}_{e,k}^T \mathbf{w}\} + \Im\{\tilde{\mathbf{h}}_{e,k}^T \mathbf{w}\} \tan \theta \end{bmatrix} \succeq \mathbf{0}, \quad \forall k, \forall l. \quad (36c)$$

B. SDP Lower Bound Solution

While the SDP upper bound formulation (36) provides some alternative solution to the original problem, SDP lower bound solution has some interesting practical significance. In particular, we do not need to relax the EH constraint in the SDP lower bound formulation. In order to derive the SDP lower bound solution of (16), we denote $N_T \times N_T$ matrix $\mathbf{W} \triangleq \mathbf{w}\mathbf{w}^H$. However, this is a strict equality constraint, which requires the matrix \mathbf{W} be of rank one. As discussed in Section III, the rank constraint on \mathbf{W} is nonconvex. In order to get around it, we replace the strict equality constraint by the inequality constraint $\mathbf{W} \succeq \mathbf{w}\mathbf{w}^H$. Thus we obtain the SDP formulation of (16) as

$$\min_{\mathbf{w}, \mathbf{W}} \text{tr}(\mathbf{W}) \quad (37a)$$

TABLE I
COMPLEXITY ORDER OF THE CONVENTIONAL
AND PROPOSED APPROACHES

Problem	Complexity Order
Problem (7)	$\ln(1/\epsilon) \sqrt{KL + K + L + (L+1)N_T^2[n_c(n_c+1) \times (KL + K + L) + n_c^3]}, n_c = \mathcal{O}((L+1)N_T^2)$
Problem (25)	$\ln(1/\epsilon) \sqrt{(6K + L + 3)n_1[(n_1+1)(6K + L) + 9K + n_1]}, n_1 = \mathcal{O}(N_T)$
Problem (34)	$\ln(1/\epsilon) \sqrt{3K + Ln_2[(n_2+1)(3K + L) + n_2^2]}, n_2 = \mathcal{O}(N_T)$
Problem (36)	$\ln(1/\epsilon) \sqrt{(6K + L + 3)n_3[(n_3+1)(6K + L) + 9K + n_3^2]}, n_3 = \mathcal{O}(N_T)$
Problem (37)	$\ln(1/\epsilon) \sqrt{(K+1)(N_T+1) + 2Kn_4[(K+1)(N_T+1)^2(N_T+n_4+1) + 4K + n_4^2]}, n_4 = \mathcal{O}(N_T^2 + N_T)$

$$\text{s.t. Constraint (16b) -- (16d),} \quad (37b)$$

$$\begin{bmatrix} \Re\{\text{tr}(\tilde{\mathbf{h}}_{e,k}^* \tilde{\mathbf{h}}_{e,k}^T \mathbf{W})\} & \sqrt{\bar{\eta}_k} \\ \sqrt{\bar{\eta}_k} & 1 \end{bmatrix} \succeq \mathbf{0}, \quad \forall k, \quad (37c)$$

$$\begin{bmatrix} \mathbf{W} & \mathbf{w} \\ \mathbf{w} & 1 \end{bmatrix} \succeq \mathbf{0}. \quad (37d)$$

SDP problems (36) and (37) can be solved efficiently using CVX [24]. Note that a rank-one \mathbf{W} always solves problem (37) optimally.

Remark 1: Note that depending on the system parameters, i.e., K, L , and N_T , SOCP may have higher complexity than SDP and vice versa. The complexity order of the conventional solution (Section III) and the proposed SOCP and SDP solutions are given in Table I based on interior-point method based solvers [24]. In this context, we would like to emphasize that the SOCP in (25) and the SDP in (36) actually have identical computational complexity. However, we note some performance gain in terms of transmit power (see Fig. 4) from the SDP solution as compared with the corresponding SOCP solution. Similar behaviour has also been observed in [18]. However, such a gain is not obvious (see Fig. 9). This actually motivated us to study both schemes for the non-convex secrecy power minimization problem in the interest of completeness for interested readers. The network designer may choose the appropriate solution depending on the available resources.

VI. CONSTRUCTIVE INTERFERENCE PRECODING FOR QAM MODULATION

As mentioned earlier, constructive interference precoding is modulation-specific. In the previous two sections, we designed secure precoding schemes for M -PSK modulation. In this section, we focus on secure constructive interference precoding for the M -QAM scheme. Fig. 3 depicts the conceptual framework of 16-QAM constellation based on binary mapping. Constructive precoding for QAM has been studied in [26] for information transmission only. Although it is notationally difficult to generalize to generic QAM [26], [27], we note that the proposed idea can be readily extended to arbitrary modulations [9]. However, defining secure regions in the presence of potential eavesdroppers based on destructive interference is significantly challenging and is still unexplored. In the following, we discuss interference exploitation schemes based

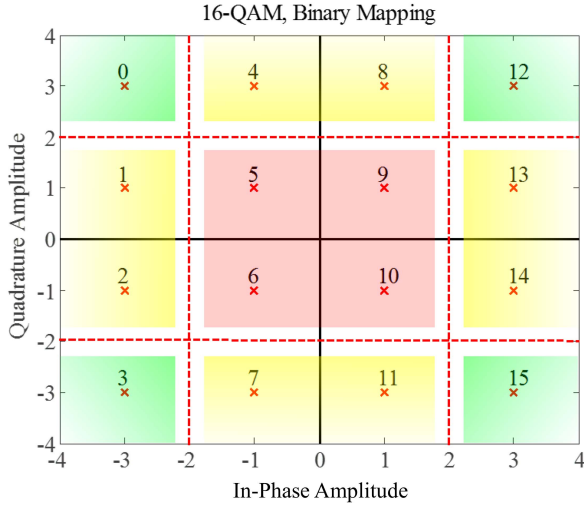


Fig. 3. Constructive framework of 16-QAM constellation based on binary mapping. The number in each box indicates the binary-coded decimal equivalent. The fading colors in the outer boxes indicate the open constructive regions while the solid color in the inner boxes indicate closed regions.

on 16-QAM for downlink secure SWIPT systems. For ease of exposition, we divide different constellation points into different color zones in Fig. 3.

Note that the transmit symbols mapped within the ‘red’ zone are surrounded by the decision boundaries and hence there is no margin for constructive precoding for transmitting these symbols to the IRs. The IRs’ SINR constraints should guarantee the exact constellation points subject to γ_d . However, the destructive regions for the ERs are still exploitable. Thus for transmit symbols within the ‘red’ zone, we define the secrecy SINR constraints as

$$C1: \Re \left\{ \tilde{\mathbf{h}}_{d,l}^T \mathbf{w} \right\} = \sigma_d \sqrt{\gamma_d} \Re \{ s_{d,l} \}, \text{ for } l = 1, \dots, L, \quad (38)$$

$$C2: \Im \left\{ \tilde{\mathbf{h}}_{d,l}^T \mathbf{w} \right\} = \sigma_d \sqrt{\gamma_d} \Im \{ s_{d,l} \}, \text{ for } l = 1, \dots, L, \quad (39)$$

$$C3: \left| \Re \left\{ \tilde{\mathbf{h}}_{e,k}^T \mathbf{w} \right\} \right| \geq \sigma_e \sqrt{\gamma_e} \Re \{ s_{d,l} \}, \text{ for } k = 1, \dots, K, \quad (40)$$

$$C4: \left| \Im \left\{ \tilde{\mathbf{h}}_{e,k}^T \mathbf{w} \right\} \right| \geq \sigma_e \sqrt{\gamma_e} \Im \{ s_{d,l} \}, \text{ for } k = 1, \dots, K. \quad (41)$$

For transmit symbols within the ‘yellow’ zone ‘4–8–7–11’, the constructive SINR constraints should aim at pushing the quadrature amplitude at the IRs away from the decision thresholds. However, the in-phase amplitude should match that of the exact constellation points. We keep the quadrature amplitude of the ERs’ received signals open along the reverse direction of the desired symbols. Thus we define the secrecy SINR constraints as

$$C1: \Re \left\{ \tilde{\mathbf{h}}_{d,l}^T \mathbf{w} \right\} = \sigma_d \sqrt{\gamma_d} \Re \{ s_{d,l} \}, \text{ for } l = 1, \dots, L, \quad (42)$$

$$C2: \left| \Im \left\{ \tilde{\mathbf{h}}_{d,l}^T \mathbf{w} \right\} \right| \geq \sigma_d \sqrt{\gamma_d} \Im \{ s_{d,l} \}, \text{ for } l = 1, \dots, L, \quad (43)$$

$$C3: \left| \Re \left\{ \tilde{\mathbf{h}}_{e,k}^T \mathbf{w} \right\} \right| \geq \sigma_e \sqrt{\gamma_e} \Re \{ s_{d,l} \}, \text{ for } k = 1, \dots, K, \quad (44)$$

$$C4: \left| \Im \left\{ \tilde{\mathbf{h}}_{e,k}^T \mathbf{w} \right\} \right| \leq \sigma_e \sqrt{\gamma_e} \Im \{ s_{d,l} \}, \text{ for } k = 1, \dots, K. \quad (45)$$

In a similar fashion, we define the constructive zone for transmit symbols within the ‘yellow’ zone ‘1–2–13–14’,

and define the secrecy SINR constraints as

$$C1: \left| \Re \left\{ \tilde{\mathbf{h}}_{d,l}^T \mathbf{w} \right\} \right| \geq \sigma_d \sqrt{\gamma_d} \Re \{ s_{d,l} \}, \text{ for } l = 1, \dots, L, \quad (46)$$

$$C2: \Im \left\{ \tilde{\mathbf{h}}_{d,l}^T \mathbf{w} \right\} = \sigma_d \sqrt{\gamma_d} \Im \{ s_{d,l} \}, \text{ for } l = 1, \dots, L, \quad (47)$$

$$C3: \left| \Re \left\{ \tilde{\mathbf{h}}_{e,k}^T \mathbf{w} \right\} \right| \leq \sigma_e \sqrt{\gamma_e} \Re \{ s_{d,l} \}, \text{ for } k = 1, \dots, K, \quad (48)$$

$$C4: \left| \Im \left\{ \tilde{\mathbf{h}}_{e,k}^T \mathbf{w} \right\} \right| \geq \sigma_e \sqrt{\gamma_e} \Im \{ s_{d,l} \}, \text{ for } k = 1, \dots, K. \quad (49)$$

For transmit symbols within the ‘green’ zones, we have the widest constructive precoding zones, and note that these are identical to the QPSK case. Following the concept discussed in Section IV for M -PSK modulation, we define the secrecy SINR constraints as

$$C1: \left| \Re \left\{ \tilde{\mathbf{h}}_{d,l}^T \mathbf{w} \right\} \right| \geq \sigma_d \sqrt{\gamma_d} \Re \{ s_{d,l} \}, \text{ for } l = 1, \dots, L, \quad (50)$$

$$C2: \left| \Im \left\{ \tilde{\mathbf{h}}_{d,l}^T \mathbf{w} \right\} \right| \geq \sigma_d \sqrt{\gamma_d} \Im \{ s_{d,l} \}, \text{ for } l = 1, \dots, L, \quad (51)$$

$$C3: \left| \Re \left\{ \tilde{\mathbf{h}}_{e,k}^T \mathbf{w} \right\} \right| \leq \sigma_e \sqrt{\gamma_e} \Re \{ s_{d,l} \}, \text{ for } k = 1, \dots, K, \quad (52)$$

$$C4: \left| \Im \left\{ \tilde{\mathbf{h}}_{e,k}^T \mathbf{w} \right\} \right| \leq \sigma_e \sqrt{\gamma_e} \Im \{ s_{d,l} \}, \text{ for } k = 1, \dots, K, \quad (53)$$

Finally, the energy harvesting constraint for QAM constellations can be bounded following similar approach as for the PSK modulation. Thus, the constructive interference-aided upper bound power minimization problem for QAM constellation is formulated as

$$\min_{\mathbf{w}, r_{1,k}, r_{2,k}} \|\mathbf{w}\|^2 \quad (54a)$$

$$\text{s.t. Constraints C1-C4,} \quad (54b)$$

$$r_{1,k} = \Re \left\{ \tilde{\mathbf{h}}_{e,k}^T \mathbf{w} \right\}, \quad \forall k, \quad (54c)$$

$$r_{2,k} = \Re \left\{ \tilde{\mathbf{h}}_{e,k}^T \mathbf{w} \right\} + \Im \left\{ \tilde{\mathbf{h}}_{e,k}^T \mathbf{w} \right\}, \quad \forall k, \quad (54d)$$

$$\left\| \begin{bmatrix} 2\sqrt{\eta_k} \\ r_{1,k} - r_{2,k} \end{bmatrix} \right\| \leq r_{1,k} + r_{2,k}, \quad \forall k, \quad (54e)$$

$$r_{1,k} \geq 0, \quad r_{2,k} \geq 0, \quad \forall k. \quad (54f)$$

Similarly, a lower bound solution can be derived for the 16-QAM scheme. However, we omit the detailed derivation of the lower bound solution for brevity.

VII. ROBUST CONSTRUCTIVE INTERFERENCE PRECODING

In the previous sections, we considered constructive interference based secure beamforming design for SWIPT with perfect CSI of all nodes available at the transmitter. However, that is a limiting assumption for many practical wireless communication systems. Although channel training is possible in the considered scenario with all the users being actively served with different services, the estimated CSI is often not perfect for various reasons. Hence in this section, we study robust CI beamforming design for scenarios when the available CSI is imperfect.

We model the imperfect CSI considering the widely used Gaussian channel error model such that the channel error vectors have circularly symmetric complex Gaussian (CSCG) distribution with norm-bounded errors. Thus, the actual channels between the BS and the l th IR can be modeled as

$$\mathbf{h}_{d,l} = \hat{\mathbf{h}}_{d,l} + \mathbf{e}_{d,l}, \quad \forall l, \quad (55)$$

and that between the BS and the k th ER can be modelled as

$$\mathbf{h}_{e,k} = \hat{\mathbf{h}}_{e,k} + \mathbf{e}_{e,k}, \quad \forall k, \quad (56)$$

where $\hat{\mathbf{h}}_{d,l}, \forall l$, and $\hat{\mathbf{h}}_{e,k}, \forall k$, denote the $N_T \times 1$ imperfect estimated CSI available at the BS and $\mathbf{e}_{d,l} \in \mathbb{C}^{N_T \times 1}, \forall l$, $\mathbf{e}_{e,k} \in \mathbb{C}^{N_T \times 1}, \forall k$, represent the channel uncertainties such that $\|\mathbf{e}_{d,l}\|^2 \leq \varepsilon_d^2, \forall l$, and $\|\mathbf{e}_{e,k}\|^2 \leq \varepsilon_e^2, \forall k$, respectively.

A. Conventional AN-Aided Robust Secure Precoding

The conventional AN-aided downlink robust secrecy power minimization problem with SINR constraints is formulated as [4]

$$\min_{\mathbf{b}_{d,l}, \mathbf{z}} \sum_{l=1}^L \|\mathbf{b}_{d,l}\|^2 + \|\mathbf{z}\|^2 \quad (57a)$$

$$\text{s.t. } \min_{\|\mathbf{e}_{d,l}\| \leq \varepsilon_d} \frac{\left| \mathbf{h}_{d,l}^T \mathbf{b}_{d,l} \right|^2}{\sum_{\substack{m=1 \\ m \neq l}}^N \left| \mathbf{h}_{d,l}^T \mathbf{b}_{d,m} \right|^2 + \left| \mathbf{h}_{d,l}^T \mathbf{z} \right|^2 + \sigma_d^2} \geq \gamma_d, \quad \forall l, \quad (57b)$$

$$\max_{\|\mathbf{e}_{e,k}\| \leq \varepsilon_e} \frac{\left| \mathbf{h}_{e,k}^T \mathbf{b}_{d,l} \right|^2}{\sum_{\substack{m=1 \\ m \neq l}}^N \left| \mathbf{h}_{e,k}^T \mathbf{b}_{d,m} \right|^2 + \left| \mathbf{h}_{e,k}^T \mathbf{z} \right|^2 + \sigma_e^2} \leq \gamma_e, \quad \forall k, \quad \forall l, \quad (57c)$$

$$\min_{\|\mathbf{e}_{e,k}\| \leq \varepsilon_e} \sum_{l=1}^L \left| \mathbf{h}_{e,k}^T \mathbf{b}_{d,l} \right|^2 + \left| \mathbf{h}_{e,k}^T \mathbf{z} \right|^2 + \sigma_e^2 \geq \bar{\eta}_k, \quad \forall k. \quad (57d)$$

Due to the spherical channel uncertainty model, constraints (57b) and (57c) actually involve infinitely many constraints which makes the problem (57) very difficult to solve. However, the inequality constraints in (57) can be transformed into convex linear matrix inequality (LMI) constraints by applying the \mathcal{S} -procedure [4, Lemma 2], and thus problem (57) can be readily solved using existing solvers. It has been proved in [21] that whenever problem (57) is feasible, the corresponding transmit precoding solution is of rank one hence optimal.

B. Constructive Interference Aided Robust Secure Precoding

In this section, we aim at constructive interference based robust secure precoding design with imperfect knowledge of all CSI, as opposed to its perfect CSI counterpart in Section IV. With the deterministic channel uncertainty model described above, we consider worst-case based robust design. Based on the problem formulation in (16) for the perfect CSI case, the CI based robust power minimization problem for SWIPT can be formulated as

$$\min_{\mathbf{w}} \|\mathbf{w}\|^2 \quad (58a)$$

$$\text{s.t. } \left| \Im \left\{ \left(\hat{\mathbf{h}}_{d,l} + \mathbf{e}_{d,l} \right)^T \mathbf{w} \right\} \right| \leq \left(\Re \left\{ \left(\hat{\mathbf{h}}_{d,l} + \mathbf{e}_{d,l} \right)^T \mathbf{w} \right\} \right. \\ \left. - \sigma_d \sqrt{\Gamma_d} \right) \tan \theta, \quad \forall \|\mathbf{e}_{d,l}\| \leq \varepsilon_d, \quad \forall l, \quad (58b)$$

$$- \Im \left\{ \left(\hat{\mathbf{h}}_{e,k} + \mathbf{e}_{e,k} \right)^T \mathbf{w} \right\} \leq \left(\Re \left\{ \left(\hat{\mathbf{h}}_{e,k} + \mathbf{e}_{e,k} \right)^T \mathbf{w} \right\} \right. \\ \left. - \sigma_e \sqrt{\Gamma_{e,k}} \right) \tan \theta, \quad \forall \|\mathbf{e}_{e,k}\| \leq \varepsilon_e, \quad \forall k, \quad (58c)$$

$$\Im \left\{ \left(\hat{\mathbf{h}}_{e,k} + \mathbf{e}_{e,k} \right)^T \mathbf{w} \right\} \geq \left(\Re \left\{ \left(\hat{\mathbf{h}}_{e,k} + \mathbf{e}_{e,k} \right)^T \mathbf{w} \right\} \right. \\ \left. - \sigma_e \sqrt{\Gamma_{e,k}} \right) \tan \theta, \quad \forall \|\mathbf{e}_{e,k}\| \leq \varepsilon_e, \quad \forall k, \quad (58d)$$

$$\left\| \left(\hat{\mathbf{h}}_{e,k} + \mathbf{e}_{e,k} \right)^T \mathbf{w} \right\| \geq \bar{\eta}_k, \quad \forall \|\mathbf{e}_{e,k}\| \leq \varepsilon_e, \quad \forall k. \quad (58e)$$

Considering the real and imaginary parts of each complex vector separately, we have

$$\tilde{\mathbf{h}}_{d,l} = \hat{\mathbf{h}}_{R,d,l} + j\hat{\mathbf{h}}_{I,d,l} + \mathbf{e}_{R,d,l} + j\mathbf{e}_{I,d,l}, \quad \forall l, \quad (59)$$

$$\mathbf{w} = \mathbf{w}_R + j\mathbf{w}_I, \quad (60)$$

where the subscripts R and I indicate the real and imaginary components of the corresponding complex notation, respectively. As such, the real part can be expressed as

$$\Re \left\{ \left(\hat{\mathbf{h}}_{d,l} + \mathbf{e}_{d,l} \right)^T \mathbf{w} \right\} \\ = \hat{\mathbf{h}}_{R,d,l}^T \mathbf{w}_R - \hat{\mathbf{h}}_{I,d,l}^T \mathbf{w}_I + \mathbf{e}_{R,d,l}^T \mathbf{w}_R - \mathbf{e}_{I,d,l}^T \mathbf{w}_I \\ = \bar{\mathbf{h}}_{d,l}^T \mathbf{w}_1 + \bar{\mathbf{e}}_{d,l}^T \mathbf{w}_1, \quad (61)$$

where $\bar{\mathbf{h}}_{d,l} \triangleq \left[\hat{\mathbf{h}}_{R,d,l}^T \quad \hat{\mathbf{h}}_{I,d,l}^T \right]^T$, $\bar{\mathbf{e}}_{d,l} \triangleq \left[\mathbf{e}_{R,d,l}^T \quad \mathbf{e}_{I,d,l}^T \right]^T$, and $\mathbf{w}_1 \triangleq \left[\mathbf{w}_R^T \quad -\mathbf{w}_I^T \right]^T$. Similarly, the imaginary component can be expressed as

$$\Im \left\{ \left(\hat{\mathbf{h}}_d + \mathbf{e}_d \right)^T \mathbf{w} \right\} \\ = \hat{\mathbf{h}}_{R,d}^T \mathbf{w}_R + \hat{\mathbf{h}}_{I,d}^T \mathbf{w}_I + \mathbf{e}_{R,d}^T \mathbf{w}_R + \mathbf{e}_{I,d}^T \mathbf{w}_I \\ = \bar{\mathbf{h}}_{d,l}^T \mathbf{w}_2 + \bar{\mathbf{e}}_{d,l}^T \mathbf{w}_2, \quad (62)$$

with $\mathbf{w}_2 \triangleq \left[\mathbf{w}_R^T \quad \mathbf{w}_I^T \right]^T$. Thus the constraint (58b) can be explicitly expressed as the following two constraints

$$\max_{\|\mathbf{e}_{d,l}\| \leq \varepsilon_d} \bar{\mathbf{h}}_{d,l}^T \mathbf{w}_2 + \bar{\mathbf{e}}_{d,l}^T \mathbf{w}_2 - \left(\bar{\mathbf{h}}_{d,l}^T \mathbf{w}_1 + \bar{\mathbf{e}}_{d,l}^T \mathbf{w}_1 \right) \tan \theta \\ + \sigma_d \sqrt{\gamma_d} \tan \theta \leq 0 \quad (63)$$

$$\max_{\|\mathbf{e}_{d,l}\| \leq \varepsilon_d} -\bar{\mathbf{h}}_{d,l}^T \mathbf{w}_2 - \bar{\mathbf{e}}_{d,l}^T \mathbf{w}_2 - \left(\bar{\mathbf{h}}_{d,l}^T \mathbf{w}_1 + \bar{\mathbf{e}}_{d,l}^T \mathbf{w}_1 \right) \tan \theta \\ + \sigma_d \sqrt{\gamma_d} \tan \theta \leq 0. \quad (64)$$

Similarly, the constraints (58c) and (58d) can be, respectively, rewritten as

$$\max_{\|\mathbf{e}_{e,k}\| \leq \varepsilon_e} -\bar{\mathbf{h}}_{e,k}^T \mathbf{w}_2 - \bar{\mathbf{e}}_{e,k}^T \mathbf{w}_2 - \left(\bar{\mathbf{h}}_{e,k}^T \mathbf{w}_1 + \bar{\mathbf{e}}_{e,k}^T \mathbf{w}_1 \right) \tan \theta \\ + \sigma_e \sqrt{\gamma_e} \tan \theta \leq 0 \quad (65)$$

$$\min_{\|\mathbf{e}_{e,k}\| \leq \varepsilon_e} \bar{\mathbf{h}}_{e,k}^T \mathbf{w}_2 + \bar{\mathbf{e}}_{e,k}^T \mathbf{w}_2 - \left(\bar{\mathbf{h}}_{e,k}^T \mathbf{w}_1 + \bar{\mathbf{e}}_{e,k}^T \mathbf{w}_1 \right) \tan \theta \\ + \sigma_e \sqrt{\gamma_e} \tan \theta \geq 0, \quad (66)$$

where $\bar{\mathbf{h}}_{e,k} \triangleq \left[\hat{\mathbf{h}}_{R,e,k}^T \quad \hat{\mathbf{h}}_{I,e,k}^T \right]^T$. On the other hand, considering the fact that $\left\| \tilde{\mathbf{h}}_{e,k}^T \mathbf{w} \right\|^2 = \Re \left\{ \tilde{\mathbf{h}}_{e,k}^T \mathbf{w} \right\}^2 + \Im \left\{ \tilde{\mathbf{h}}_{e,k}^T \mathbf{w} \right\}^2$, the energy harvesting constraints (58e) can be expressed as

$$\bar{\mathbf{e}}_{e,k}^T (\mathbf{W}_1 + \mathbf{W}_2) \bar{\mathbf{e}}_{e,k} + 2\bar{\mathbf{e}}_{e,k}^T (\mathbf{W}_1 + \mathbf{W}_2) \bar{\mathbf{h}}_{e,k} \\ + \bar{\mathbf{h}}_{e,k}^T (\mathbf{W}_1 + \mathbf{W}_2) \bar{\mathbf{h}}_{e,k} \geq \bar{\eta}_k, \quad \forall k, \\ \|\mathbf{e}_{e,k}\| \leq \varepsilon_e, \quad \forall k, \quad (67)$$

where $\mathbf{W}_1 \triangleq \mathbf{w}_1 \mathbf{w}_1^T$ and $\mathbf{W}_2 \triangleq \mathbf{w}_2 \mathbf{w}_2^T$. Applying \mathcal{S} -procedure [22], the constraint (67) can be expressed as the following LMI:

$$\begin{bmatrix} \mu_{e,k} \mathbf{I}_{N_T} + \mathbf{W}_1 + \mathbf{W}_2 & (\mathbf{W}_1 + \mathbf{W}_2) \bar{\mathbf{h}}_{e,k} \\ \bar{\mathbf{h}}_{e,k}^T (\mathbf{W}_1 + \mathbf{W}_2) & \kappa_{e,k} \end{bmatrix} \succeq \mathbf{0}, \quad \forall k. \quad (68)$$

Here, $\mu_{e,k}, k = 1, \dots, K$, are the associated slack variables and $\kappa_{e,k} \triangleq \bar{\mathbf{h}}_{e,k}^T (\mathbf{W}_1 + \mathbf{W}_2) \bar{\mathbf{h}}_{e,k} - \bar{\eta}_k - \mu_{e,k} \varepsilon_e^2$.

By replacing the CSI error bounds in these constraints, the robust problem (58) can be reformulated as

$$\min_{\mathbf{w}_1, \mathbf{w}_2, \mathbf{W}_1, \mathbf{W}_2, \{\mu_{e,k}\}} \|\mathbf{w}_2\|^2 \quad (69a)$$

$$\text{s.t. } \bar{\mathbf{h}}_{d,l}^T \mathbf{w}_2 - \bar{\mathbf{h}}_{d,l}^T \mathbf{w}_1 \tan \theta + \varepsilon_d \|\mathbf{w}_2 - \mathbf{w}_1 \tan \theta\| \\ + \sigma_d \sqrt{\gamma_d} \leq 0 \quad (69b)$$

$$- \bar{\mathbf{h}}_{d,l}^T \mathbf{w}_2 - \bar{\mathbf{h}}_{d,l}^T \mathbf{w}_1 \tan \theta + \varepsilon_d \|\mathbf{w}_2 + \mathbf{w}_1 \tan \theta\| \\ + \sigma_d \sqrt{\gamma_d} \leq 0, \quad (69c)$$

$$- \bar{\mathbf{h}}_{e,k}^T \mathbf{w}_2 - \bar{\mathbf{h}}_{e,k}^T \mathbf{w}_1 \tan \theta - \varepsilon_e \|\mathbf{w}_2 + \mathbf{w}_1\| \tan \theta \\ + \sigma_e \sqrt{\gamma_e} \leq 0 \quad (69d)$$

$$\bar{\mathbf{h}}_{e,k}^T \mathbf{w}_2 + \bar{\mathbf{h}}_{e,k}^T \mathbf{w}_1 \tan \theta - \varepsilon_e \|\mathbf{w}_2 + \mathbf{w}_1\| \tan \theta \\ + \sigma_e \sqrt{\gamma_e} \geq 0, \quad (69e)$$

$$\text{Constraints (68) satisfied,} \quad (69f)$$

$$\begin{bmatrix} \mathbf{W}_1 & \mathbf{w}_1 \\ \mathbf{w}_1 & 1 \end{bmatrix} \succeq \mathbf{0}, \quad \begin{bmatrix} \mathbf{W}_2 & \mathbf{w}_2 \\ \mathbf{w}_2 & 1 \end{bmatrix} \succeq \mathbf{0}, \quad (69g)$$

$$\text{rank}(\mathbf{W}_1) = 1, \quad \text{rank}(\mathbf{W}_2) = 1. \quad (69h)$$

Now, the problem (69) can be efficiently solved after rank-relaxation using existing solvers [24]. The solution is optimal if $\text{rank}(\mathbf{W}_1) = 1$ and $\text{rank}(\mathbf{W}_2) = 1$, in which case it holds true that $\mathbf{W}_1 = \mathbf{w}_1 * \mathbf{w}_1^T$ and $\mathbf{W}_2 = \mathbf{w}_2 * \mathbf{w}_2^T$. Otherwise, one may need to resort to an alternative approach, for example randomization, to construct rank-one \mathbf{W}_1 and \mathbf{W}_2 . Interested readers are referred to [28] and [29] for different rank-one solution construction procedures.

C. Robust Power Minimization for QAM Constellation

In this subsection, we study the robust counterpart of the 16-QAM scheme developed in Section VI. The constructive interference-aided upper bound power minimization problem with imperfect CSI for QAM constellation can be formulated as

$$\min_{\mathbf{w}_1, \mathbf{w}_2, \mathbf{W}_1, \mathbf{W}_2, \{\mu_{e,k}\}} \|\mathbf{w}_2\|^2 \quad (70a)$$

$$\text{s.t. } \bar{\mathbf{h}}_{d,l}^T \mathbf{w}_1 + \bar{\mathbf{e}}_{d,l}^T \mathbf{w}_1 \stackrel{\leq}{\stackrel{\geq}{\leq}} \sigma_d \sqrt{\gamma_d} \Re\{s_{d,l}\}, \quad \forall l, \quad (70b)$$

$$\bar{\mathbf{h}}_{d,l}^T \mathbf{w}_2 + \bar{\mathbf{e}}_{d,l}^T \mathbf{w}_2 \stackrel{\leq}{\stackrel{\geq}{\leq}} \sigma_d \sqrt{\gamma_d} \Im\{s_{d,l}\}, \quad \forall l, \quad (70c)$$

$$\bar{\mathbf{h}}_{e,k}^T \mathbf{w}_1 + \bar{\mathbf{e}}_{e,k}^T \mathbf{w}_1 \stackrel{\leq}{\stackrel{\geq}{\leq}} \sigma_d \sqrt{\gamma_d} \Re\{s_{d,l}\}, \quad \forall l, \quad \forall k, \quad (70d)$$

$$\bar{\mathbf{h}}_{e,k}^T \mathbf{w}_2 + \bar{\mathbf{e}}_{e,k}^T \mathbf{w}_2 \stackrel{\leq}{\stackrel{\geq}{\leq}} \sigma_d \sqrt{\gamma_d} \Im\{s_{d,l}\}, \quad \forall l, \quad \forall k, \quad (70e)$$

$$\text{Constraints (68), (69g) satisfied,} \quad (70f)$$

$$\text{rank}(\mathbf{W}_1) = 1, \quad \text{rank}(\mathbf{W}_2) = 1. \quad (70g)$$

TABLE II
LIST OF ALGORITHMS COMPARED

Legend	Algorithm
No Eve CSI (conv)	Conventional isotropic beamforming without eavesdropper's CSI proposed in [19].
No Eve CSI (cons)	Constructive isotropic beamforming without eavesdropper's CSI, i.e., problem (16a)-(16b) ignoring the remaining constraints.
Full CSI (conv)	Conventional AN-aided secure beamforming scheme discussed in Section III [3].
Cons UB	Constructive AN-aided upper bound solution developed in Section IV-A.
Cons UB	Constructive AN-aided lower bound solution developed in Section IV-B.
SDP UB	SDP formulation of the constructive AN-aided upper bound solution derived in Section V-A.
SDP LB	SDP formulation of the constructive AN-aided lower bound solution derived in Section V-B.
16-QAM	Constructive AN-aided multi-level modulation for 16-QAM upper bound solution derived in Section VI.
Conv Rob Prec	Conventional robust secure beamforming scheme for SWIPT [21, Problem (16)].
Const Rob Prec	CI-based robust precoding derived in Section VII-B.

where $\stackrel{\leq}{\stackrel{\geq}{\leq}}$ suggests the appropriate direction of the inequalities based on the transmit symbol mapping shown in the constellation diagram in Fig. 3 and in the explicit expressions in (38) - (53). Substituting the error bounds, the problem (70) is solvable using off-the-shelf convex optimization toolboxes after rank-relaxation.

VIII. SIMULATION RESULTS

In this section, we present numerical simulation results to evaluate the performance of the proposed constructive interference based PLS algorithms for wireless data and energy integrated communications in a MISO wiretap channel. Unless otherwise specified, QPSK and 16-QAM are the modulation schemes considered. All the estimated channel vectors are generated as independent and identically distributed complex Gaussian random variables with mean zero and the TGN path-loss model for urban cellular environment is adopted considering a path-loss exponent of 2.7 [30]. Noise power level is set to $\sigma_d = \sigma_e = 1$ in all simulations. All simulation results are averaged over 2000 independent channel realizations, unless explicitly mentioned. In the following simulations, we compare the performance of the proposed approaches with that of the conventional AN-aided precoding scheme in [31] as the benchmark. The legends in the figures are defined in Table II.

We first demonstrate the performance of the non-robust algorithms with perfect CSI. Fig. 4 shows the average instantaneous transmit power for the algorithms versus the SINR threshold at the IRs with $N_T = 8, L = 2, K = 4, \Gamma_e = -10$ (dB), and $\eta = -5$ (dBW). It can be seen from Fig. 4 that the constructive interference based schemes significantly outperform the conventional beamforming schemes in terms of transmit power. In particular, the proposed schemes for QPSK modulation require down to 60% of power compared to the conventional counterpart (plotted with pentagon point marker). For example, the proposed schemes yield almost 10dB gain for QPSK modulation at 20dB SINR target. The respective gains

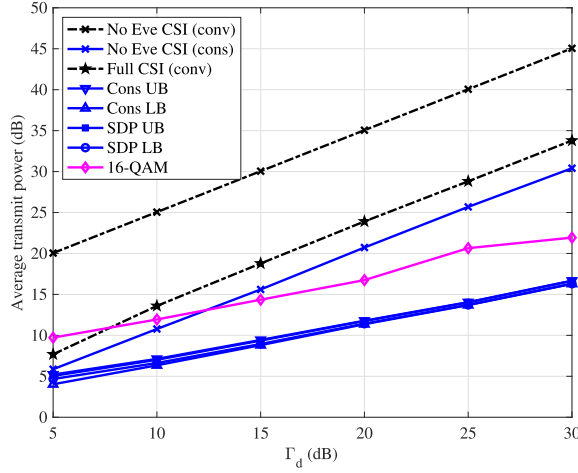


Fig. 4. Transmit power P_T versus required SINR at IR Γ_d with $N_T = 8, L = 2, K = 4, \Gamma_e = -10$ (dB), and $\eta = -5$ (dBW).

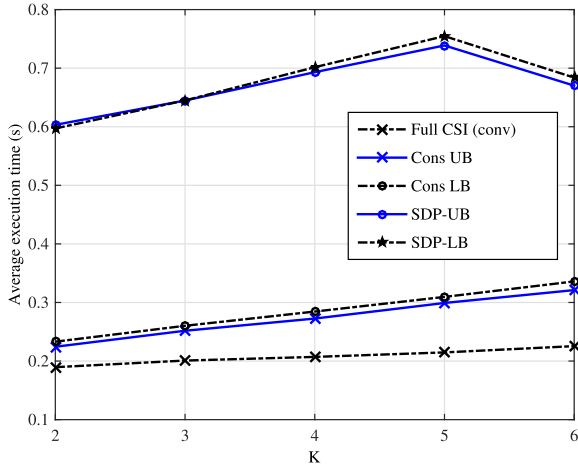


Fig. 5. Average time complexity per optimization versus the number of eavesdroppers K with $N_T = 8, L = 2, \Gamma_d = 15$ (dB), $\Gamma_e = -10$ (dB), and $\eta = -5$ (dBW).

still persists for 16-QAM at 12 dB SINR. In addition, while the target SINR increases, the gap between the conventional and the proposed schemes keeps increasing, indicating even better performance at higher SINR targets. Another important observation is that the performance gap between the proposed upper and lower bound schemes are really small, which indicates that the proposed bounds are indeed tight. On the other hand, the ‘No Eve CSI’ schemes require significantly higher power, which is vastly dependent on the total transmit power budget. Interestingly, even without imposing the eavesdropping constraints explicitly, the constructive interference based ‘No Eve CSI’ scheme outperforms the conventional isotropic beamforming scheme proposed in [19].

Note that in Fig. 4, we have compared the transmit power requirements of the proposed constructive interference based schemes with that of the relevant conventional schemes in [3] and [4]. For the conventional schemes, we plot average expected transmit power while for the proposed schemes, we plot the average instantaneous transmit power. However, the conventional schemes are normally performed per each

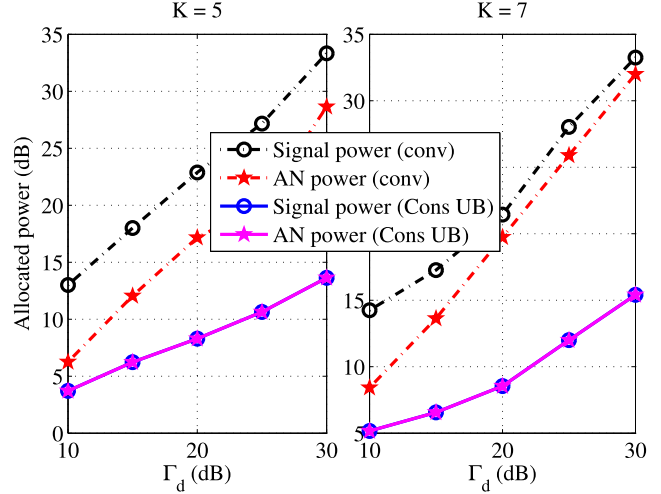


Fig. 6. Instantaneous power allocation between information and AN signals versus required SINR at IR Γ_d with $N_T = 8, L = 2, K = 5, 7, \Gamma_e = -10$ (dB), and $\eta = -5$ (dBW).

transmission frame while the proposed schemes are performed for every symbol period. Now, in order to provide a fairer comparison, we show the average time complexity of the algorithms per optimization. In Fig. 5, we show the average execution time of the proposed constructive interference based schemes as well as the conventional scheme in [3] and [4]. The results in Fig. 5 are produced in an iMac with a 4.2 GHz Intel Core i7 processor and 64 GB 2400 MHz DDR4 RAM running on MacOS High Sierra version 10.13.4. We solved the optimization problems using the Matlab based solver CVX [24]. Clearly, the average execution time of the proposed SOCP schemes is comparable to that of the conventional schemes. Note that the average execution time of the SDP schemes is relatively higher due to the additional constraints replacing the energy harvesting constraint.

Overall, our proposed approaches require a higher symbol-by-symbol optimization complexity, and this is shared with all interference exploitation approaches compared to conventional schemes [7]–[9], [11]–[13]. We note however, that this complexity involves the BS in the downlink transmission, where computational resources are far more accessible, and in fact, it was shown in [32] that there are significant complexity savings at the MU receivers. Clearly, this complexity increase at the BS is well motivated by the significant performance gains from the interference exploitation approach.

In the next couple of examples, we will have a closer look into the transmit power distribution between the information and the AN signals to get more insights. Fig. 6 shows the instantaneous power allocation between information ($\|\mathbf{b}_d\|^2$) and AN signals ($\|\mathbf{z}\|^2$) versus required SINR at IR Γ_d with $N_T = 8, L = 2, K = 5, 7, \Gamma_e = -10$ (dB), and $\eta = -5$ (dBW), whereas Fig. 7 depicts the same versus eavesdropping constraints at the ERs Γ_e with $N_T = 8, L = 3, K = 5, \Gamma_d = 20$ (dB), $\eta = -5$ (dBW), and QPSK modulation. In both cases, one can notice that the power allocated to AN in the conventional scheme is significantly higher compared to that in the constructive interference schemes. This observation

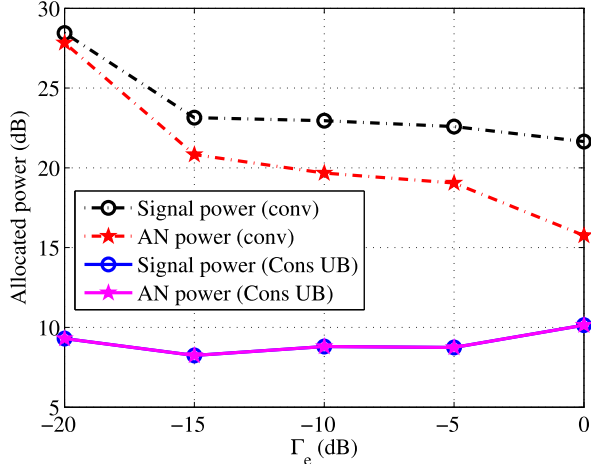


Fig. 7. Instantaneous power allocation between information and AN signals versus required SINR at ER Γ_e with $N_T = 8$, $L = 3$, $K = 5$, $\Gamma_d = 20$ (dB), and $\eta = -5$ (dBW).

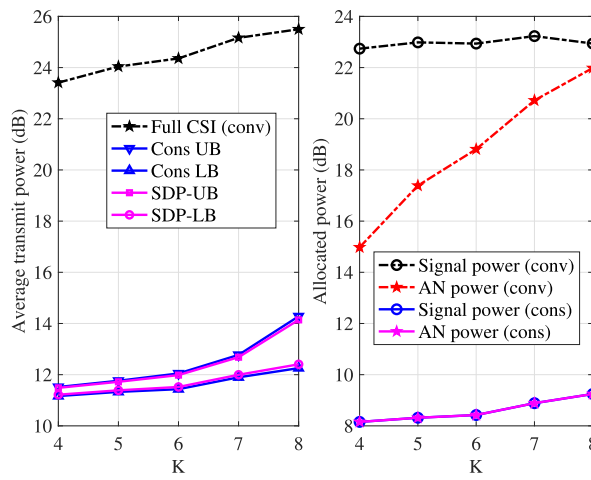


Fig. 8. Transmit power P_T versus the number of eavesdroppers with $N_T = 8$, $L = 2$, $\Gamma_d = 20$ (dB), $\Gamma_e = -10$ (dB), and $\eta = -5$ (dBW).

demonstrates the effectiveness of constructive interference schemes. As derived in (11), it is the constructive interference/AN power that allows guaranteeing the SINR requirements at the legitimate receivers at lower transmit power. Note that the gap between the signal and the AN power in the conventional scheme reduces for an increased number of users (e.g., $K = 7$), as also observed in [31]. However, an interesting observation is that the constructive interference schemes split the transmit power almost equally between information and AN beams. From Fig. 7, it can also be revealed that with relaxed eavesdropping constraints (increasing Γ_e), less power is invested on AN in the conventional scheme to block weaker eavesdropping attempts. On the other hand, power splitting remains the same in constructive interference schemes even with relaxed eavesdropping constraints.

Now we are interested in observing the transmit power requirements of the algorithms with increasing number of potential eavesdroppers. Note that in our system model, eavesdropping attempts are exposed by the legitimate ERs. Hence,

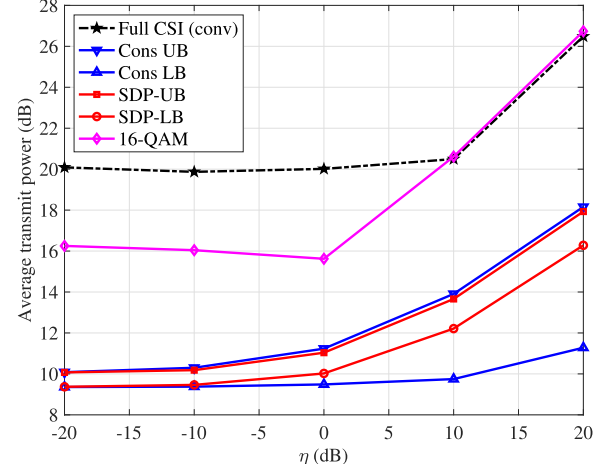


Fig. 9. Transmit power P_T versus energy harvesting threshold at the ERs η with $N_T = 8$, $L = 3$, $K = 5$, $\Gamma_d = 15$ (dB), and $\Gamma_e = -10$ (dB).

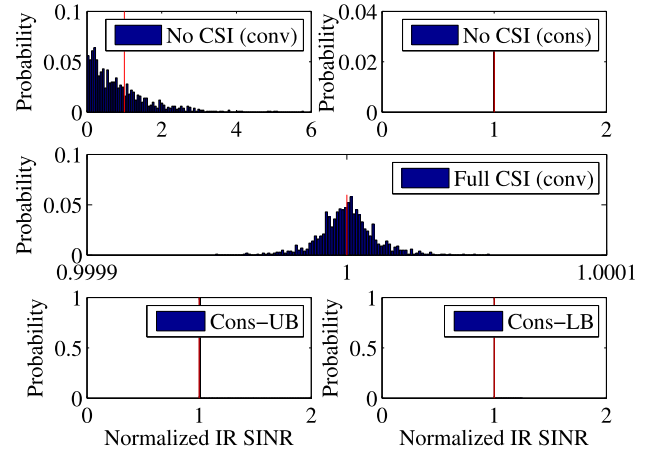


Fig. 10. Normalized histogram of the average IR SINR with $N_T = 8$, $L = 3$, $K = 5$, $\Gamma_d = 10$ (dB), $\Gamma_e = -5$ (dB), and $\eta = 15$ (dBW).

an increase in the number of eavesdropping ERs emphatically increases the number of energy harvesting and secrecy constraints. Fig. 8 plots the transmit power of the various designs, as well as the power allocation between information and AN signals versus the number of ERs with $N_T = 8$, $L = 2$, $\Gamma_d = 20$ (dB), $\Gamma_e = -10$ (dB), $\eta = -5$ (dBW), and QPSK modulation. Again, the proposed schemes exhibit superior performance. It is no surprise to observe that with increasing K , the transmit power of all the algorithms keeps increasing, since increasing number of ER means more eavesdropping threats.

Let us now focus on the energy harvesting performance of the proposed algorithms as compared with the conventional schemes proposed in [33]. In Fig. 9, we plot the instantaneous transmit powers for the algorithms versus the energy harvesting threshold at the ERs averaged over channel realizations. This time we set $N_T = 8$, $L = 3$, $K = 5$, $\Gamma_d = 15$ (dB), and $\Gamma_e = -10$ (dB). It can be observed from the results in Fig. 9 that the required transmit power in the conventional and the 16-QAM schemes is almost invariant at low EH requirements although it sharply increases after 10 dBW. This happens

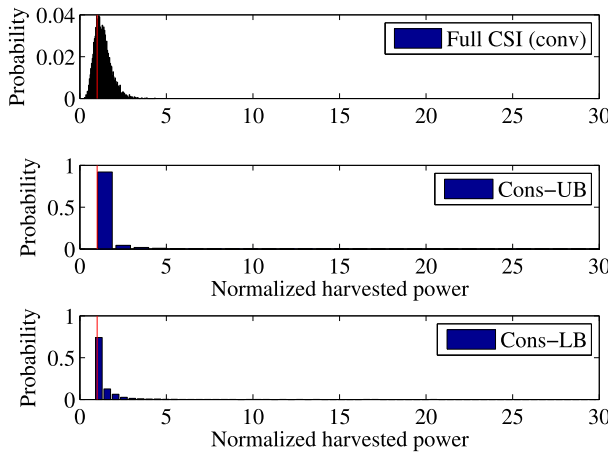


Fig. 11. Normalized histogram of harvested power at the ERs with $N_T = 8, L = 3, K = 5, \Gamma_d = 10 (dB), $\Gamma_e = -5 (dB), and $\eta = 15 (dBW).$$$

because the SINR thresholds requirements overshadow the EH requirements at low EH threshold for these two schemes. On the other hand, the proposed upper and lower bound schemes exhibit a gradual increase in transmit power for QPSK modulation with increasing EH requirements.

Next, we demonstrate the efficiency of the proposed constructive interference based secure beamforming schemes by examining their achievable instantaneous received SINR at the IRs. Fig. 10 shows the histograms of the achievable SINRs normalized by the thresholds on per symbol basis with $N_T = 8, L = 3, K = 5, \Gamma_d = 10 (dB), $\Gamma_e = -5 (dB), and $\eta = 15 (dBW). It can be observed from this figure that although the conventional SINR constraint (7b) guarantees the average IR SINR requirement, the same may not be guaranteed for every symbol period. As indicated by the histograms of the conventional schemes, the achievable received SINR has a Gaussian distribution and almost in 50% of the cases the SINR requirement may not be satisfied on an instantaneous basis. Indeed, this may potentially result in outages for the respective users. In contrast, the proposed constructive interference based schemes always guarantee the SINR requirements. Thus the proposed schemes are great candidates for systems with stringent SINR requirements.$$$

A similar observation can be drawn by the histogram of the instantaneous harvested power normalized by the thresholds at the ERs in Fig. 11 with $N_T = 8, L = 3, K = 5, \Gamma_d = 10 (dB), $\Gamma_e = -5 (dB), $\eta = 15 (dBW), and QPSK modulation. Similar to the legitimate ERs' SINR case (Fig. 10), the conventional average EH constraint based approach violates the instantaneous EH constraints in many cases. On the other hand, the proposed constructive interference based schemes guarantee each constraint for every symbol period.$$$

Finally, we investigate the performance of the proposed robust algorithms with imperfect CSI available at the transmitter. Fig. 12 illustrates the average instantaneous transmit power versus the radius of the channel uncertainty region of the legitimate IRs ε_d with $N_T = 8, L = 3, \Gamma_d = 15 (dB), $\Gamma_e = -10 (dB), $\eta = -5 (dBW), and $\varepsilon_e = 0.1$ for robust beamforming design. Results in Fig. 12 demonstrate that even$$$

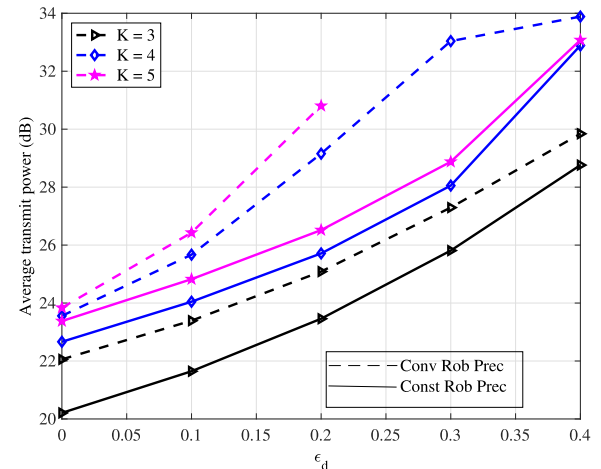


Fig. 12. Transmit power P_T versus the radius of the channel uncertainty region of the legitimate IRs ε_d with $N_T = 8, L = 3, \Gamma_d = 15 (dB), $\Gamma_e = -10 (dB), $\eta = -5 (dBW), and $\varepsilon_e = 0.1$ for robust beamforming design.$$$

with imperfect CSI the proposed constructive interference schemes outperform conventional schemes. While the relative comparison of transmit power for the conventional and the proposed constructive interference schemes follows a similar pattern as observed in the perfect CSI case, an increase in the uncertainty in channel estimation results in higher transmit power for both schemes in order to guarantee the same QoS level. This is obvious since increased channel uncertainty region effectively means more inaccurate channel information. Also, securing information against increased number of eavesdroppers demands additional transmit power.

IX. CONCLUSIONS

We proposed interference exploitation approaches for AN-aided secure beamforming in simultaneous information and energy transfer systems. We studied the downlink transmit power minimization problem under secrecy SINR and energy harvesting constraints considering both perfect and imperfect CSI at the BS. In the proposed schemes, multiuser interference as well as AN are designed to be constructive to the IRs and disruptive to the potential eavesdropping ERs. Additionally, the AN is exploited as a vehicle for energy transfer. Thus the AN plays a triple role in the proposed schemes in contrast to its double role in conventional SWIPT systems. Simulation results demonstrated that the proposed schemes significantly reduce transmit power by proactively exploiting interference and AN power.

REFERENCES

- [1] R. Zhang and C. K. Ho, "MIMO broadcasting for simultaneous wireless information and power transfer," *IEEE Trans. Wireless Commun.*, vol. 12, no. 5, pp. 1989–2001, May 2013.
- [2] E. Hossain and M. Hasan, "5G cellular: Key enabling technologies and research challenges," *IEEE Instrum. Meas. Mag.*, vol. 18, no. 3, pp. 11–21, Jun. 2015.
- [3] L. Liu, R. Zhang, and K.-C. Chua, "Secrecy wireless information and power transfer with MISO beamforming," *IEEE Trans. Signal Process.*, vol. 62, no. 7, pp. 1850–1863, Apr. 2014.

[4] M. R. A. Khandaker and K.-K. Wong, "Masked beamforming in the presence of energy-harvesting eavesdroppers," *IEEE Trans. Inf. Forensics Security*, vol. 10, no. 1, pp. 40–54, Jan. 2015.

[5] C. Masouros, T. Ratnarajah, M. Sellathurai, C. Papadias, and A. Shukla, "Known interference in wireless communications: A limiting factor or a potential source of green signal power?" *IEEE Commun. Mag.*, vol. 51, pp. 162–171, Oct. 2013.

[6] G. Zheng, I. Krikidis, C. Masouros, S. Timotheou, D.-A. Toumpakaris, and Z. Ding, "Rethinking the role of interference in wireless networks," *IEEE Commun. Mag.*, vol. 52, no. 11, pp. 152–158, Nov. 2014.

[7] C. Masouros and E. Alsusa, "Dynamic linear precoding for the exploitation of known interference in MIMO broadcast systems," *IEEE Trans. Wireless Commun.*, vol. 8, no. 3, pp. 1396–1404, Mar. 2009.

[8] C. Masouros, "Correlation rotation linear precoding for MIMO broadcast communications," *IEEE Trans. Signal Process.*, vol. 59, no. 1, pp. 252–262, Jan. 2011.

[9] C. Masouros and G. Zheng, "Exploiting known interference as green signal power for downlink beamforming optimization," *IEEE Trans. Signal Process.*, vol. 63, no. 14, pp. 3628–3640, Jul. 2015.

[10] C. Masouros, M. Sellathurai, and T. Ratnarajah, "Vector perturbation based on symbol scaling for limited feedback MISO downlinks," *IEEE Trans. Signal Process.*, vol. 62, no. 3, pp. 562–571, Feb. 2014.

[11] M. Alodeh, S. Chatzinotas, and B. Ottersten, "Constructive multiuser interference in symbol level precoding for the MISO downlink channel," *IEEE Trans. Signal Process.*, vol. 63, no. 9, pp. 2239–2252, May 2015.

[12] M. R. A. Khandaker, C. Masouros, and K.-K. Wong, "Constructive interference based secure precoding," in *Proc. IEEE ISIT*, Aachen, Germany, Jun. 2017, pp. 2875–2879.

[13] M. R. A. Khandaker, C. Masouros, and K.-K. Wong, "Constructive interference based secure precoding: A new dimension in physical layer security," *IEEE Trans. Inf. Forensics Security*, vol. 17, no. 9, pp. 2256–2268, Sep. 2018.

[14] C. Li, J. Wang, F.-C. Zheng, J. M. Cioffi, and L. Yang, "Overhearing based cooperation for two-cell network with asymmetric uplink-downlink traffics," *IEEE Trans. Signal Inf. Process. Netw.*, vol. 2, pp. 350–361, Sep. 2016.

[15] C. Li, H. J. Yang, F. Sun, J. M. Cioffi, and L. Yang, "Adaptive overhearing in two-way multi-antenna relay channels," *IEEE Signal Process. Lett.*, vol. 23, no. 1, pp. 117–120, Jan. 2016.

[16] C. Li, S. Zhang, P. Liu, F. Sun, J. M. Cioffi, and L. Yang, "Overhearing protocol design exploiting intercell interference in cooperative green networks," *IEEE Trans. Veh. Technol.*, vol. 65, no. 1, pp. 441–446, Jan. 2016.

[17] C. Li, H. J. Yang, F. Sun, J. M. Cioffi, and L. Yang, "Multiuser overhearing for cooperative two-way multiantenna relays," *IEEE Trans. Veh. Technol.*, vol. 65, no. 5, pp. 3796–3802, May 2016.

[18] S. Timotheou, G. Zheng, C. Masouros, and I. Krikidis, "Exploiting constructive interference for simultaneous wireless information and power transfer in multiuser downlink systems," *IEEE J. Sel. Areas Commun.*, vol. 34, no. 5, pp. 1772–1784, May 2016.

[19] S. Goel and R. Negi, "Guaranteeing secrecy using artificial noise," *IEEE Trans. Wireless Commun.*, vol. 7, no. 6, pp. 2180–2189, Jun. 2008.

[20] Q. Li and W.-K. Ma, "Spatially selective artificial-noise aided transmit optimization for MISO multi-eyes secrecy rate maximization," *IEEE Trans. Signal Process.*, vol. 61, no. 10, pp. 2704–2717, May 2013.

[21] M. R. A. Khandaker and K.-K. Wong, "Robust secrecy beamforming with energy-harvesting eavesdroppers," *IEEE Wireless Commun. Lett.*, vol. 4, no. 1, pp. 10–13, Feb. 2015.

[22] S. Boyd and L. Vandenberghe, *Convex Optimization*. Cambridge, U.K.: Cambridge Univ. Press, 2004.

[23] N. P. Le, "Throughput analysis of power-beacon assisted energy harvesting wireless systems over non-identical Nakagami- n fading channels," *IEEE Commun. Lett.*, vol. 22, no. 4, pp. 840–843, Apr. 2018.

[24] M. Grant and S. Boyd. *CVX: MATLAB Software for Disciplined Convex Programming (Web Page and Software)*, Version 2.1. Accessed: Dec. 2017. [Online]. Available: <http://cvxr.com/cvx>

[25] E. Alsusa and C. Masouros, "Adaptive code allocation for interference management on the downlink of DS-CDMA systems," *IEEE Trans. Wireless Commun.*, vol. 7, no. 7, pp. 2420–2424, Jul. 2008.

[26] M. Alodeh, S. Chatzinotas, and B. Ottersten, "Constructive interference through symbol level precoding for multi-level modulation," in *Proc. IEEE Globecom*, San Diego, CA, USA, Dec. 2015, pp. 1–6.

[27] A. Li and C. Masouros, "Exploiting constructive mutual coupling in P2P MIMO by analog-digital phase alignment," *IEEE Trans. Wireless Commun.*, vol. 16, no. 3, pp. 1948–1962, Mar. 2017.

[28] N. D. Sidiropoulos, T. N. Davidson, and Z.-Q. Luo, "Transmit beamforming for physical-layer multicasting," *IEEE Trans. Signal Process.*, vol. 54, no. 6, pp. 2239–2251, Jun. 2006.

[29] M. R. A. Khandaker and K.-K. Wong, "SWIPT in MISO multicasting systems," *IEEE Wireless Commun. Lett.*, vol. 3, no. 3, pp. 277–280, Jun. 2014.

[30] *TGn Channel Models*, document IEEE 802.11-03/940r4, IEEE P802.11 Wireless LANs, May 2004.

[31] W.-C. Liao, T.-H. Chang, W.-K. Ma, and C.-Y. Chi, "QoS-based transmit beamforming in the presence of eavesdroppers: An optimized artificial-noise-aided approach," *IEEE Trans. Signal Process.*, vol. 59, no. 3, pp. 1202–1216, Mar. 2011.

[32] K. L. Law, C. Masouros, and M. Pesavento, "Transmit precoding for interference exploitation in the underlay cognitive radio Z-channel," *IEEE Trans. Signal Process.*, vol. 65, no. 14, pp. 3617–3631, Jul. 2017.

[33] M. R. A. Khandaker and K.-K. Wong, "Max-min energy based robust secure beamforming for SWIPT," in *Proc. IEEE ICC*, London, U.K., Jun. 2015, pp. 166–171.



Muhammad R. A. Khandaker (S'10–M'13–SM'18) received the B.Sc. degree (Hons.) in computer science and engineering from Jahangirnagar University, Dhaka, Bangladesh, in 2006, the M.Sc. degree in telecommunications engineering from East West University, Dhaka, in 2007, and the Ph.D. degree in electrical and computer engineering from Curtin University, Australia, in 2013.

He was a Post-Doctoral Researcher with the Department of Electronic and Electrical Engineering, University College London, U.K., from 2013 to

2018. He is currently an Assistant Professor with the School of Engineering and Physical Sciences, Heriot-Watt University, U.K. He also worked in a number of academic positions in Bangladesh. He was a recipient of the Curtin International Postgraduate Research Scholarship for his Ph.D. study in 2009. He was a recipient of the Best Paper Award in the 16th IEEE Asia-Pacific Conference on Communications, Auckland, New Zealand, in 2010. He is an Associate Editor of the IEEE ACCESS and the EURASIP Journal on Wireless Communications and Networking. He also served as the Managing Guest Editor for Physical Communication (Elsevier), special issue on Self-Optimizing Cognitive Radio Technologies. He is currently serving as the Lead Guest Editor for the EURASIP Journal on Wireless Communications and Networking, special issue on Heterogeneous Cloud Radio Access Networks.



Christos Masouros (M'06–SM'14) received the Diploma degree in electrical and computer engineering from the University of Patras, Greece, in 2004, and the M.Sc. degree by research and the Ph.D. degree in electrical and electronic engineering from The University of Manchester, U.K., in 2006 and 2009, respectively. In 2008, he was a Research Intern with Philips Research Labs, U.K. From 2009 to 2010, he was a Research Associate with The University of Manchester and from 2010 to 2012, he was a Research Fellow with Queen's University Belfast.

He has held a Royal Academy of Engineering Research Fellowship from 2011 to 2016.

He is currently a Senior Lecturer with the Communications and Information Systems Research Group, Department of Electronic and Electrical Engineering, University College London. His research interests lie in the field of wireless communications and signal processing with particular focus on green communications, large-scale antenna systems, cognitive radio, interference mitigation techniques for MIMO, and multicarrier communications. He was a recipient of the Best Paper Award at the IEEE Globecom conference in 2015. He has been recognized as an Exemplary Editor of the IEEE COMMUNICATIONS LETTERS and an Exemplary Reviewer of the IEEE TRANSACTIONS ON COMMUNICATIONS. He is an Associate Editor of the IEEE COMMUNICATIONS LETTERS, and a Guest Editor of the IEEE JOURNAL ON SELECTED TOPICS IN SIGNAL PROCESSING issue Exploiting Interference towards Energy Efficient and Secure Wireless Communications.



Kai-Kit Wong (M'01–SM'08–F'16) received the B.Eng., M.Phil., and Ph.D. degrees from The Hong Kong University of Science and Technology, Hong Kong, in 1996, 1998, and 2001, respectively, all in Electrical and Electronic Engineering. He is currently a Professor of wireless communications with the Department of Electronic and Electrical Engineering, University College London, U.K. He is fellow of the IET. He is Senior Editor of the IEEE COMMUNICATIONS LETTERS and the IEEE WIRELESS COMMUNICATIONS LETTERS.



Stelios Timotheou (S'04–M'10–SM'17) received the B.Sc. degree from the Electrical and Computer Engineering School, National Technical University of Athens, and the M.Sc. and Ph.D. degrees from the Electrical and Electronic Engineering Department, Imperial College London. In previous appointments, he was a Research Associate with KIOS, a Visiting Lecturer with the Department of Electrical and Computer Engineering, University of Cyprus, and a Post-Doctoral Researcher with the Computer Laboratory of the University of Cambridge. He is currently an Assistant Professor with the Department of Electrical and Computer Engineering and a Faculty Member with the KIOS Research and Innovation Center of Excellence, University of Cyprus.

His research focuses on analyzing data and making informed decisions in challenging environments, with the purpose of enhancing efficiency and delivering new capabilities in situational awareness and decision making. Toward this direction, he develops customized, real-time, distributed, and cooperative methodologies and algorithms, drawing on theory from mathematical optimization, machine learning, statistical data processing, and computational intelligence. The main application area of his research is critical infrastructure systems, with emphasis on intelligent transportation systems and wireless communications.

Dr. Timotheou was a recipient of the 2017 Cyprus Young Researcher in Physical Sciences & Engineering Award from the Cyprus Research Promotion Foundation.